Journal of Geosciences and Geomatics, 2019, Vol. 7, No. 3, 112-133
Available online at http://pubs.sciepub.com/jgg/7/3/3
Published by Science and Education Publishing
DOI:10.12691/jgg-7-3-3

Lithogenic Concentrations of Useful Elements and Residual Mineralization Indices in the Weathering Products Derived from Mineralized Rocks in Meïganga (Central Cameroon)

Tchaptchet. T.W.[1,*], Tematio. P.[1], Njiki. C.C.[1], Guimapi. T.N.[1], Hapi. F.[1], Tiomo. I.[1], Tchuenkam. D.B.[1], Momo. N.N.M.[2]

[1]Department of Earth Science, University of Dschang, P.O. Box. 67, Dschang, Cameroon
[2]Institut de Recherche Géologique et Minière (IRGM), Yaoundé, Nkolbissong, Cameroon
*Corresponding author: christiantchapy@yahoo.com

Received April 07, 2019; Revised May 17, 2019; Accepted June 10, 2019

Abstract This paper focuses on the use of morphological, mineralogical and geochemical characterization of weathering profiles from mineralized rocks in Meïganga, a locality in the South-East of Cameroon. It is aimed at assessing weathering processes that induced the lithogenic concentrations of useful elements, and eventually residual mineralization indices in weathered products. Seven weathering profiles derived from four distinct mineralized rocks (micaschists, orthogneiss, granite, and quartzite veins) were studied. The profiles exhibit shallow weathered A/B/C or A/C soil profiles with a moderate thickness (less than 4m). Minerals identified in the weathered products in decreasing contents (%) were: quartz (60.3-93.9), kaolinite (0.8-22.3), phlogopite (0.2-15.3), goethite (1.9-13.0), hematite (0.5-8.5), halloysite (0.2-4.6) and smectite (0.5-4.3). The SiO_2 contents generally decrease upward in these weathering profiles, except for those from granitic parent rock. Inversely, Al_2O_3, Fe_2O_3 and TiO_2 contents increase upward, except for the weathering profiles from granite and orthogneiss. Alkaline and alkaline earths are more or less completely exported during weathering. Chemical weathering parameters have revealed intense rocks weathering in Meïganga, resulting to the important accumulation of quartz in association with 1:1 clay minerals. Trace elements that prevail in these weathered products arranged in decreasing order of abundance include: S, Ba, Sr, Zr, Cr, V, Zn, Rb, Ni, Y, Sb, Cu, Pb, Li, Co, Ga, Nb, Th, Sc, Cs, Hf, Sn, U, Mo, and W. The most significant useful elements identified in these weathered products are arranged in decreasing order of abundance include: Zr, Cr, V, Sb, U, Cu, Nb, Hf, Mo, and W. The weathered products present a CI-chondrite normalized pattern of REEs characterized by the fractionation of HREEs relative to LREEs. The accumulation of trace elements (Ga, W, Y, Sn, Hf, Nb, Cu, Sc, V, Zn, Cr, Sb, Pb, Ni, Co, Li, Mo, Th, Rb, Cs, U, Zr and Ba) and REEs in the weathered products of Meïganga has been attributed to the effects of weathering. The main host minerals are the residual primary minerals (epidote, apatite, pyrite, titanite, zircon, or opaque minerals) and the newly formed secondary minerals (phlogopite, hematite, goethite, kaolinite and smectite). Correlation matrices between useful elements (Cr, Mo, U, V, Nb, Zr, Sb, Hf and W) and major oxides (Fe_2O_3, TiO_2, P_2O_5 and Al_2O_3) indicates a strong affinity (>0.80), suggesting the trace elements are noble metals. Therefore, major oxides used as tracers for residual mineralization indices are: Al_2O_3 (Nb, Mo, U, W and Hf), Fe_2O_3 (Mo, Cr, V, Zr, Hf and Sb), P_2O_3 (U, Hf and Sb), and TiO_2 (Nb, Zr, V and Cr). In the Meïganga soil profiles, mineralization indices could be assigned to W, V, Hf, Nb, Mo, Cr, Sb and U.

Keywords: *weathering products, useful elements, residual mineralization indices; African shear zone, Meïganga, central Cameroon*

Cite This Article: Tchaptchet. T.W., Tematio. P., Njiki. C.C., Guimapi. T.N., Hapi. F., Tiomo. I., Tchuenkam. D.B., and Momo. N.N.M., "Lithogenic Concentrations of Useful Elements and Residual Mineralization Indices in the Weathering Products Derived from Mineralized Rocks in Meïganga (Central Cameroon)." *Journal of Geosciences and Geomatics*, vol. 7, no. 3 (2019): 112-133. doi: 10.12691/jgg-7-3-3.

1. Introduction

Rock type plays a fundamental role in the degree and intensity of weathering, as well as the mobilization and concentration of chemical elements on the Earth surface [1,2]. The intensity of weathering also depends on a number of factors including climate and the tectonic activities. Meïganga is located in the Adamawa region of Cameroon and lies on the North-Eastern part of the Central African Fold Belt (CAFB) in Cameroon. This

mobile belt is known to have been highly affected by tectonic movements during the Pan African orogeny (600-500 Ma) leading to a complex metamorphism and to the formation of different grades of metamorphic rocks [3-9]. The intensity of tectonic activities contributed to the rocks weathering and thus allowed the accumulation of trace metals in the weathering products at different elevations. The North-Eastern part of the CAFB in Cameroon as other orogenic belts is characterized by an important mineralization potential [9-20] which resulted from hydrothermalism. However, previous works on metallogenic products are mainly based on the use of basement rocks and alluvial deposits for prospection [10,11,13-19,21,22]. Meanwhile, the use of residual deposits derived from weathered products to prospect mineral and ore deposits is not well-documented [23,24]. Weathering processes and related chemical elements mobilization are premonitory precursors of some chemical element accumulation in weathered products and the occurrence of residual ores deposits on the Earth surface [11,12,25,26]. In this paper, we intend to propose a model for the future of mineralization identified in fresh rocks during weathering processes in Meïganga. This work will allow to clarify the implication of weathering intensity and trends into the processes inducing lithogenic concentrations of useful elements into the weathering products in tropical area which belong to anorogeny belt. Hence, we propose a model of residual ore deposits prospection based on major oxides used as indicators of useful elements mineralization indices in weathering products. Therefore, seven weathering profiles developed on four distinct mineralized rocks in Meïganga have been used to trace the pathway of mineral and chemical elements mobilization in one hand and their evolution in the related weathering products. Furthermore, we determine the weathering trends and intensity as well as the amount of useful elements mobilized.

2. Geomorphology and Geological Setting of Meïganga

The study area is located in the Adamaoua plateau (Central Cameroon). It covers a surface area of about 12245 km^2. Geomorphologically, the Meïganga area is situated at the Southern border of the Adamaoua plateau which corresponds to a wide-range of lateritic paleo- surfaces with a mean altitude of 1,400m*asl* (Figure 1A and Figure 1B). The Digital Elevation Model (DEM) shows three main morphological landscapes in Meïganga (Figure 1C): the Upper, the Intermediate and the Lower landscapes.

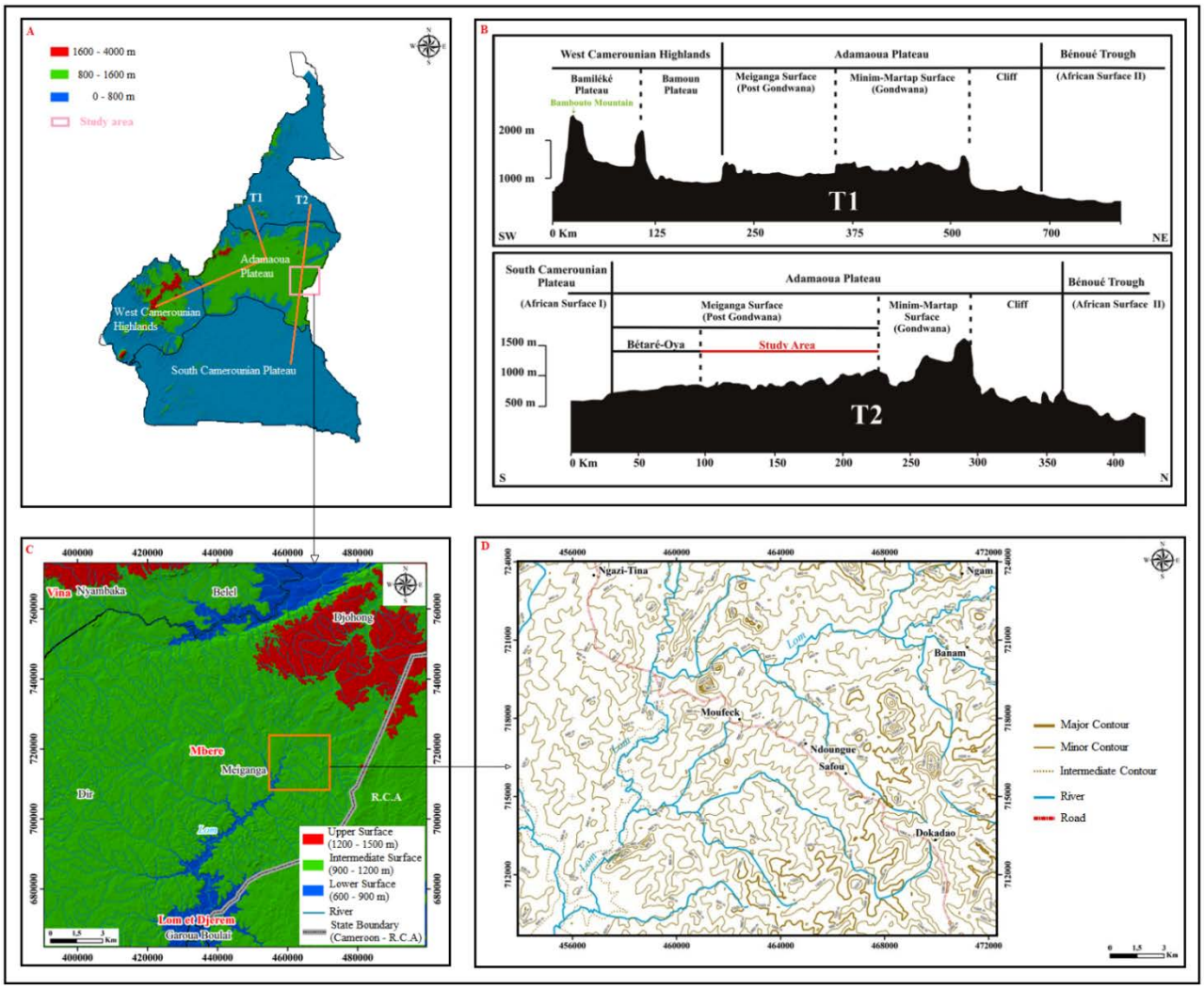

Figure 1. Geomorphology and Location map of the Meïganga study area. A. The main lateritic plateaus of Cameroon. B. Cross sections along the Adamaoua plateau. C. Digital elevation model (DEM) of the Meïganga study area. D. Topographic map of the Meïganga study site

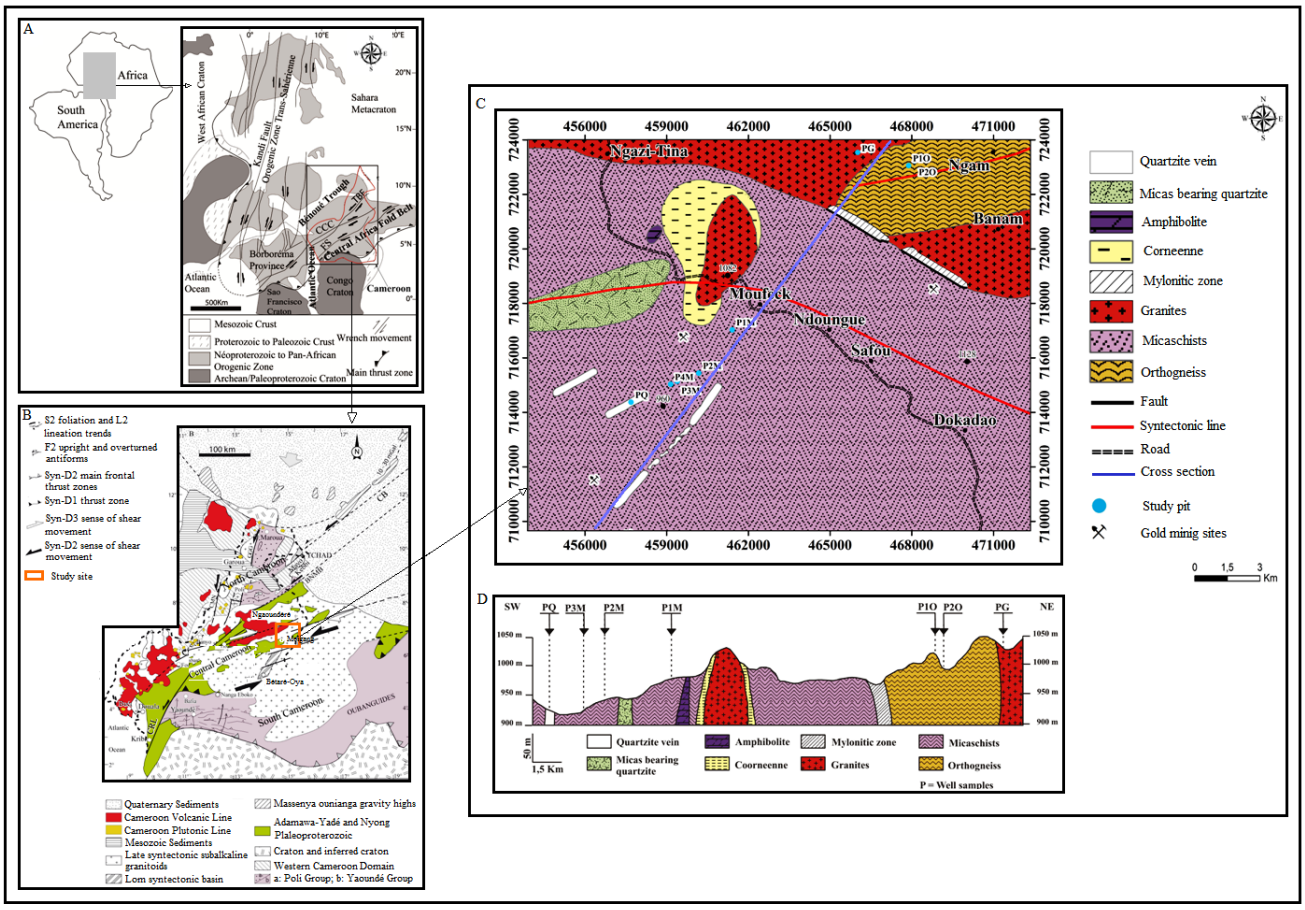

Figure 2. Geological sketch of the Meïganga study area. A. Thrust belt between São Francisco, Congo and West African Cratons. B. Map of Cameroon showing the Cameroon section of the African shear zone (CSASZ). C. Geological map of the Meïganga study area. D. Synthesizing cross section of geology in the study area

The *Upper landscape*, with altitudes ranging between 1,200 and 1,500m*asl*, is observed in the North-Eastern and the Northern borders of the study area. It covers a surface area of approximately 1,325 km^2, representing 10.8% of the study area.

The *Intermediate landscape*, with altitudes ranging between 900 and 1,200m*asl*, covers a surface area of 10,044 km^2 and represents 82.0% of the study area. Thus, it represents the most wide-spread landscape and may be considered as the representative landscape of the Meïganga study area.

The *Lower landscape*, with altitudes ranging between 600 and 900m*asl*, is located exclusively along the *Lom River* valley in the South, and the *Vina River* valley in the North-East. It covers a surface area of 876 km^2, representing 7.2% of the study area.

The Meïganga study area belongs to the north-eastern part of the CAFB in Cameroon. This belt is considered as resulting from the convergence of three main cratonic blocs: the São Francisco- Congo Craton (SFCC), the West African Craton (WAC) and the Saharan meta-craton Bloc (Figure 2A and Figure 2B). The rocks in this area were subjected to different degrees of metamorphism, leading to the formation of metamorphic rocks of different grades [3,4,5,6,8,9,27]. In Meïganga, different metamorphic rocks have been described (Figure 2C) including: orthogneiss, amphibolites, micaschists, mica bearing quartzites, granites, corneenes, quartzite veins and mylonitic zones [3,4,28,29]. A synthesis of the cross-section of the geology of Meïganga (Figure 2D) has helped to establish the geological history of the study area. First, the Meïganga region was affected by syn-, late- and post-tectonic granitic intrusions hosted in metamorphic rocks [19,30]. Metamorphic host rocks comprise amphibolites, meta-sediments made up of micaschists and quartzites (700-1000Ma) and orthogneiss dating back to 2.1 Ga. The entire host rocks were reworked during the Pan African orogeny [3,8,9,19,28,29,31,32]. Th-U-Pb monazite dating indicates an emplacement age of around 615±27 Ma for granitic intrusions in this region and 575±8 Ma for the mica-bearing granites.

Previous studies in this area have shown that mineralizations are hosted within micaschists, orthogneiss, granites, and the quartzite veins which correspond to the basement rocks [9,10,13,14,21,22]. Mineral associations in these rocks have been reported by [3,28,29]. They noted that orthogneiss are made up of quartz, K-feldspar, plagioclase, biotite, amphibole, and opaque minerals, (apatite, zircon, titanite and pyrites) occurring as accessory minerals. Micaschists are made up of quartz, biotite and feldspar, with calcite, epidote, pyrite and opaque minerals as accessory minerals. Granites also contain quartz, K-feldspar, plagioclase, biotite and muscovite, with apatite, titanite, zircon and pyrites as accessory minerals, whereas chlorite, calcite, epidote and opaque minerals behave like secondary minerals resulting from hydrothermal weathering. The quartzite veins contain mainly quartz and muscovite, but biotite, plagioclase and opaque minerals can be present in small amounts. Micaschists and the quartzite veins in this area

have been reported to be mineralization bearing such as graphite (C), gold (Au), Zinc (Zn), Copper (Cu), lead (Pb), Barium (Ba), tungsten (W), Arsenic (As), uranium (U) and diamond (C) [10,13,22]. Granites were also admitted to be holders of gold (Au), sapphire (Al_2O_3), monazite [(Ce, La, Nd, Th)PO_4], silver (Ag), molybdenum (Mo), lead (Pb), tin (Sn), manganese (Mn), arsenic (As) and uranium (U) [13,14]. The presence of pyrite (FeS_2) in mica schists, granites and orthogneiss may be indicative of their substantial mineralizations [9,21,22].

3. Methods of Study

Seven soil profiles representing the main weathering mantles developed on four mineralized rocks were hand-dug and described macroscopically [33]. A total of twenty-seven soil samples were collected and crushed into fine powder (<2mm) for mineral and geochemical analysis. Mineral identifications were performed by the X-ray diffraction (XRD) method using PW 1800 diffractometer upon the following conditions: cobalt anode (K-Alpha), wavelength, λ:1.79 Å, scanning speed: 0.033°/s, scan range: 5-78°, drive axis 2θ. The relative amounts of minerals were quantified from X-ray diffraction patterns using the Rietveld refinement method [20]. Major element contents were carried out by X-ray Fluorescence (XRF) using a Panalytical Axios advanced PW 4400 fluorescence spectrometer. Trace and Rare Earths (RE) Elements were determined by Inductively Coupled Plasma-Mass Spectrometry (ICP-MS) after three progressive acid [34]. The REEs fractionation was performed using fractionation index ***a***; the Ce/Ce* and $(La/Yb)_N$ ratios, as well as the REEs normalization relative to CI-chondrite [35].

The weathering trends and intensity were assessed using the chemical index of alteration (CIA; [36]); the Weathering Index of Parker (WIP; [37]); the Total reserve in bases (TRB; [23]); and the index of lateritization (IOL; [38]). Correlations between major, trace and RE elements were performed using the Spearman correlation function [39] combined with the Principal Components Analysis (PCA) of the outcome correlation matrix. Indeed, the PCA is a powerful statistical method that helps to reduce the number of appropriate variables describing variation within a set of data. This is done by assessing linear combinations of the variables (chemical elements), which describes the distributions and relationships of the data. Ideally, each component might have been used to describe the geological process such as weathering and mineralization [40,41]. In this study, factor analysis with PCA performed using Statistica (v. 7.0) software, allowed reducing the size of the space of the variables [42]. Thus, the PCA main goal is to provide a small number of independent factors (principal components) which synthesize the associations between variables. The first factor (Fact 1) explains a major part of the total variance of the data set, and the other successive factors explain a smaller part of the remaining variance. The different factors are then related to common processes that affect the variables. The number of significant principal components for interpretation is selected on the basis of the Kaiser criterion with an eigenvalue higher than 1 [24] and a total of variance equal to or higher than 85%.

4. Results

4.1. Macroscopic Organization of the Meïganga Weathering Mantles

Soil profiles for weathering mantles developed on micaschists (P1M, P2M and P3M), orthogneiss (P1O and P2O), granite (PG), and quartzite vein (PQ) are presented in Figure 3.

4.1.1. Weathering Mantle Developed on Micaschists

The representative soil profiles are developed at different locations and altitudes; a profile on the top of an interfluve at 949 m (P1M), a profile on a lowland at 934 m (P2M) and a profile on the footslope (P3M) at 931 m (Figure 3A). Randomly disperse rock fragments are frequently noted in lowlands and footslopes. Almost every soils profiles in this group embody less than 4m thick shallow weathered A/B/C soils profiles. In these soil profiles, the surface horizon A corresponds to a moderate thick (20-30 cm thick) soils horizon made up of dark brown (10YR2/1) silty clayey to sandy-clayey soil matrix with crumbly structure. It grades downward to the underlying subsurface horizon B_{11}, made up of a fairly to strongly thick (70 to 130 cm thick) soil horizon with light reddish brown (2.5YR7/4) silty clayey soil matrix with fine polyhedral to coarse prismatic structure. In P1M and P3M, the subsurface horizon B_{11} grades downwards to a weathered horizon BC characterized by dark yellowish brown (10YR4/6), sandy-clayey and massive saprolitic boulders embedded into reddish yellow (7.5YR7/8) and sandy loam soil matrix with coarse polyhedric structure. In this weathered horizon BC, the amount and size of the saprolitic boulders increase with depth and demarcate an almost continuous weathered horizon C. In all these soils profiles, the continuous weathered horizon C is made up of yellowish brown (10YR5/6) and more or less weathered rocks volumes embedded into a pinkish white (7.5YR8/2), clayey silt, massive and continuous saprolitic material.

4.1.2. Weathering Mantle Developed on Orthogneiss

The two profiles are located upslope (P1O) and downslope (P2O) at altitudes of 954 m and 951 m, respectively. Both profiles exhibit less than 4m thick shallow weathered A/B/C-type soil profiles. The surface horizon A corresponds to a slightly and moderately thick (10 to 30 cm thick) soil horizon with dark yellowish brown (10YR3/6) sandy loam and crumbly soil matrix, containing more or less weathered rock fragments. It grades downwards to the underlying brighter subsurface horizon B, made up of less than 100 cm thick soil horizon, with yellow (10YR8/8) and clayey sandy soil matrix, displaying a polyhedric to prismatic structure. In P1O, the subsurface horizon B grades downward to a weathered horizon BC, with yellowish brown (10YR5/6), sandy loam and massive saprolitic boulders embedded into reddish yellow (7.5YR7/8) and sandy loam soil matrix with coarse polyhedric structure. The amount and size of the saprolitic boulders increase with depth and demarcates an almost continuous weathered C horizon. In both soil profiles, the continuous weathered horizon C display a more or less weathered rock volumes embedded in a pinkish white (7.5YR8/2), clayey silty, massive and continuous saprolitic material.

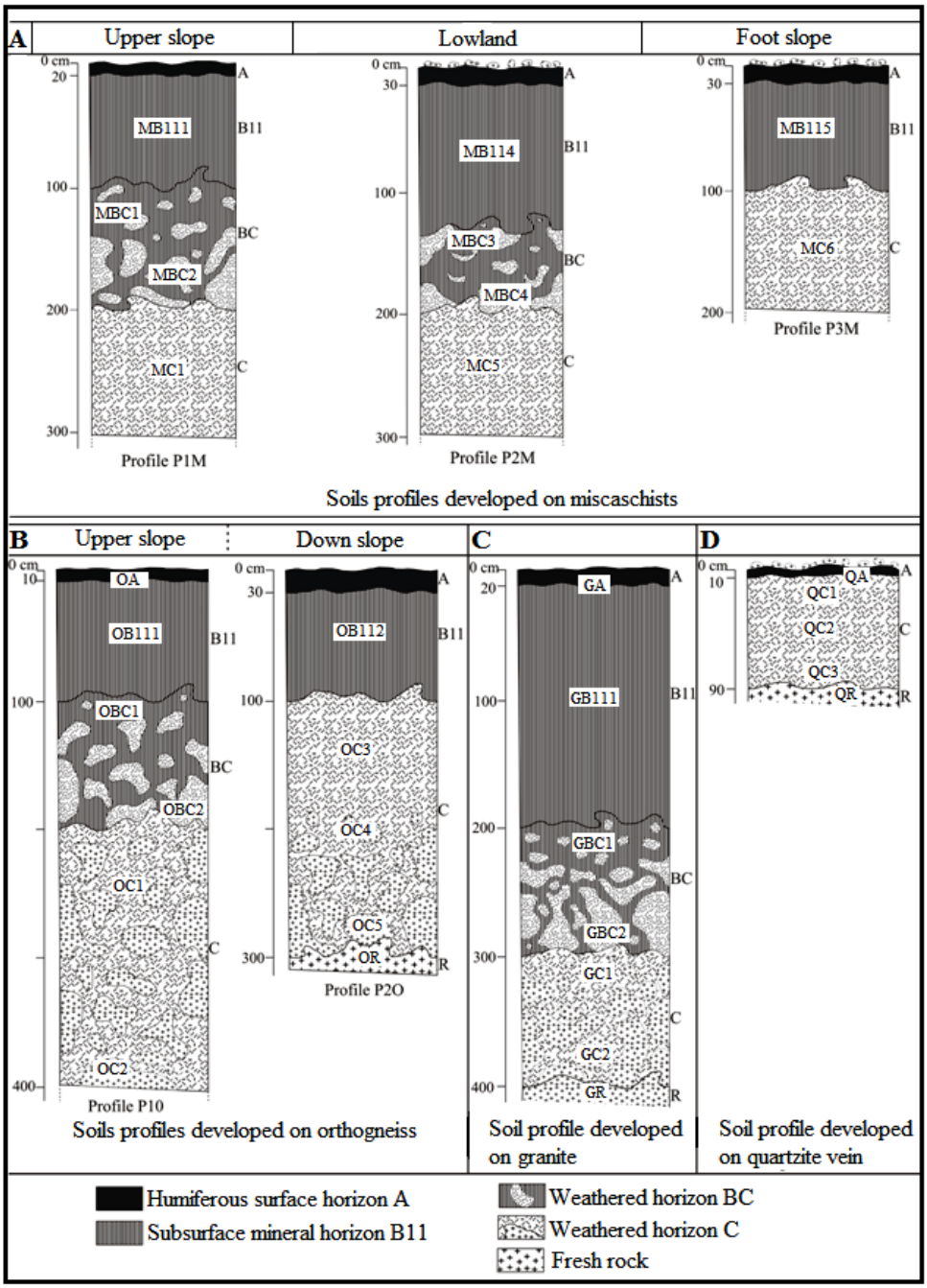

Figure 3. Macroscopic organization of the Meïganga Soils profiles. Soils profiles developed on, A. Micaschist; B. Orthogneiss; C. Granite; D. Quartzite veins

4.1.3. Weathering Mantle Developed on Granite

The soil profile (PG) developed on granite is located on the foot of a rocky hill at an altitude of 974 m. It exhibits a 4 m thick shallow weathered A/B/C-type soil profile. The surface horizon A is made up of a moderate thick (20 cm) soil with dark grey (7.5YR3/1), sandy loam and crumbly soil matrix containing more or less weathered rock fragments. The surface A horizon grades downward to the underlying brighter subsurface horizon B with 190 cm thick soil horizon, displaying a yellow (10YR8/6), sandy-clayey and polyhedric soil matrix. The subsurface horizon B grades downwards to the weathered horizon BC with yellowish brown (10YR5/6), sandy loam and massive saprolitic boulders embedded into a soil matrix made up of a yellow (10YR8/6), sandy-clayey and polyhedric fine earth. The saprolitic boulders become larger with depth and exhibit a continuous weathered horizon C with more or less weathered rock fragments embedded in pinkish grey (5YR7/2) saprolitic materials.

4.1.4. Weathering Mantle Developed on Quartzite Veins

The soil profile (PQ) developed on quartzite veins is located on a slightly undulating landscape with randomly dispersed rock fragments at an altitude of 933 m. It exhibits a 90 cm thick shallow weathered A/C-type soils profile.

The surface horizon A is a thin (10cm thick) soil horizon with dark-yellowish brown (10YR3/6), sandy loam and crumbly soil matrix with fragments of quartzite. It grades downwards to a continuous weathered horizon C with more or less weathered saprolitic materials with abundant quartzite fragments.

To summarize, the weathering mantles in Meïganga exhibit shallow weathered A/B/C or A/C-type soil profiles with a thickness not exceeding 4 m. Almost all these weathering mantles differentiate moderately to thin surface horizon A (10-30 cm), that lies on a thick subsurface horizon B (70 to 130 cm), with the exception of those developed on quartzite veins, where the surface horizon A is lying directly on the weathered horizon C. The weathering levels are made up of dominantly moderate thick (80 to 300 cm thick) weathered horizon C locally linked to the subsurface horizon B by a relatively thin (50-100 cm) weathered horizon BC. Moreover, all the weathering profiles in this area are located between altitudes 930 and 975 m, that represents the *Intermediate landscape* of the Meïganga study area.

4.2. Mineral Contents and Their Distribution in the Study Area

Mineral contents and their distribution in the seven soils profiles are summarized in Figure 4.

4.2.1. Weathering Profiles Developed on Micaschists

The mineral association of weathered profiles developed on mica schist is made up of the following minerals in decreasing abundance (%); quartz (67.0-89.2), kaolinite (8.2-12.7), goethite (1.9-13.0), hematite (0.5-8.5), phlogopite (0.7-5.0), and smectite (0.7-4.3). the abundances of quartz and kaolinite increases upward in all the soil profiles with increasing ratios of 0.07% and 0.29%, respectively. The content of hematite increases upward only in P1M (maximum increasing ratio: 1.38), while P2M and P3M profiles are characterized by alternating increasing and decreasing values. On the other hand, phlogopite and smectite abundances decrease upward the soil profiles with maximum decreasing values of 0.85% and 0.77%, respectively. Goethite is observed only in P2M soil profile.

4.2.2. Weathering Profiles Developed on Orthogneiss

The mineral association of weathered profiles developed on orthogneiss includes the following minerals in decreasing abundance (%); quartz (71.5-95.5), kaolinite (3.8-22.3), halloysite (0.2-4.6), goethite (2.0-2.3), and smectite (0.7). Quartz contents generally increases upward (maximum increasing ratio 0.13), while kaolinite and halloysite contents decrease upward, with the maximum decreasing ratios of 0.49 and 0.89, respectively. Smectite appears in a very low amount (0.7%) in the surface A horizon in profile P1O. On other hand, goethite presents a complex characteristic in profile P2O with alternation of increasing and decreasing contents.

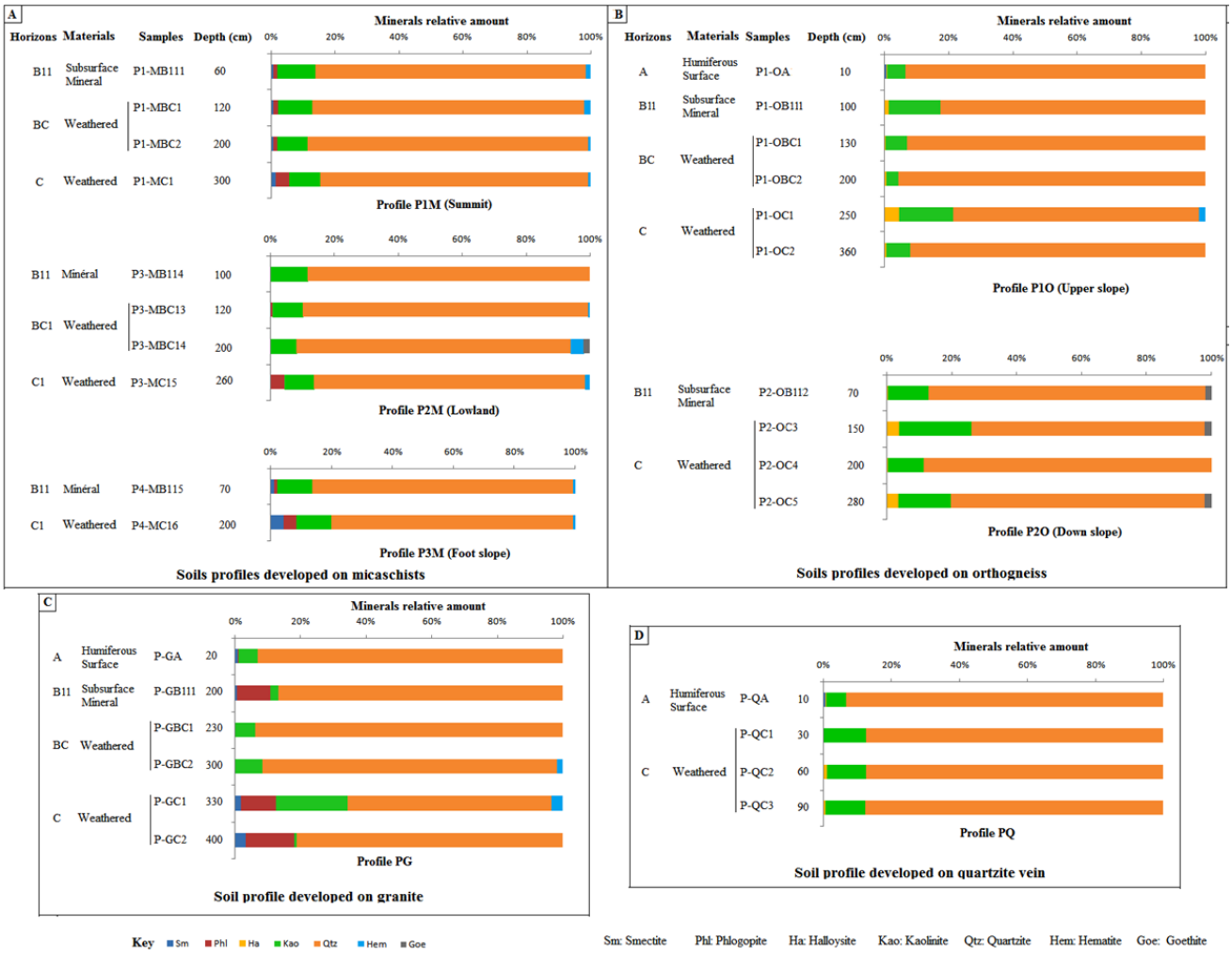

Figure 4. Minerals detected by XRD and their relative contents in the Meïganga weathered products

4.2.3. Weathering Profile Developed on Granite

The mineral association of weathered profiles developed on granite includes the following minerals in decreasing abundance (%); quartz (60.3-93.9), kaolinite (0.8-21.1), phlogopite (0.2-15.3), hematite (1.7-3.2), and smectite (0.5-3.2). Quartz and kaolinite contents increase upward, with the maximum increasing ratios of 0.13 and 25.38, respectively. In contrary, hematite, phlogopite and smectite contents decrease upward, with the maximum decreasing ratios of 0.47, 0.99, and 0.47, respectively.

4.2.4. Weathering Profile Developed on Quartzite Veins

The mineral association of weathered profiles developed on quartzite veins include the following minerals in decreasing abundance (%); quartz (87.1 - 93.2), kaolinite (5.9-12.4), halloysite (0.2-1.2), smectite (0.7) and hematite (0.5). Smectite and hematite are observed in a low amount (0.7% and 0.5%, respectively) in the surface A horizon and the weathered horizon C respectively. Quartz contents increases upwards with maximum increasing ratio of 0.07.

Table 1. Major elements contents and some weathering parameters in the Meïganga weathering profiles; TRB, total reserve in bases; CIA, chemical index of alteration; IOL, index of lateritization; Ki, silica exportation ratio; WIP, Weathering index of Parker

					Major elements in percent of oxides (%)										Chemical weathering indices				
	Soils profiles	Horizons	Samples	Depth (cm)	SiO_2	Al_2O_3	Fe_2O_3	TiO_2	MnO	MgO	CaO	Na_2O	K_2O	P_2O_5	TRB (mg/kg)	CIA (%)	IOL (%)	Ki	WIP
Weathered profiles on micaschist	**P1M**	B11	P1-MB111	60	66.2	15.7	8.5	0.7	0.1	0.0	0.0	0.1	1.6	0.0	37	90	27	4	13
		BC1	P1-MBC11	120	67.2	14.6	7.5	1.0	0.1	0.3	0.1	0.1	1.3	0.1	49	90	25	5	11
			P1-MBC12	200	70.3	13.0	7.4	0.9	0.0	0.3	0.1	0.1	1.3	0.1	46	89	22	5	11
		C1	P1-MC11	300	67.2	14.1	6.8	0.7	0.1	2.4	0.2	2.5	1.9	0.1	245	76	24	5	32
	P2M	B11	P2-MB114	100	69.4	13.2	6.6	0.9	0.1	0.3	0.0	0.1	1.2	0.1	42	90	22	5	10
		BC1	P2-MBC13	120	74.0	11.0	6.9	0.9	0.0	0.2	0.0	0.0	1.1	0.0	37	89	19	7	10
			P2-MBC14	200	67.0	7.9	18.9	0.3	0.0	0.0	0.0	0.0	0.5	0.2	12	92	29	9	4
		C1	P2-MC15	260	75.9	14.0	2.9	0.2	0.0	0.4	0.0	0.1	3.8	0.0	103	77	18	5	31
	P3M	B11	P3-MB115	70	63.6	15.0	10.1	1.2	0.2	0.4	0.0	0.1	1.4	0.1	54	90	28	4	12
		C1	P3-MC16	200	62.4	16.2	8.5	0.8	0.1	2.2	0.1	1.1	2.2	0.1	192	83	28	4	26
		Rock	**Micaschist**	-	71.4	13.5	5.7	0.5	0.0	0.7	0.2	3.1	3.1	0.1	206	68	21	5	44
Weathered profiles on orthogneiss	**P1O**	B11	P1-OB121	100	53.7	19.7	13.9	0.8	0.0	0.4	0.0	0.1	2.6	0.1	79	84	39	3	22
		BC2	P1-OBC21	130	69.2	16.3	4.9	0.5	0.0	0.2	0.0	0.2	2.4	0.1	68	82	23	4	20
			P1-OBC22	200	74.8	13.4	4.2	0.3	0.1	0.2	0.0	0.2	2.9	0.1	75	77	19	6	25
		C2	P1-OC21	250	63.5	18.6	8.0	1.0	0.0	0.3	0.0	0.2	3.6	0.1	98	80	30	3	30
			P1-OC22	280	76.1	13.3	3.0	0.3	0.0	0.1	0.0	0.2	3.5	0.1	88	74	18	6	30
	P2O	B11	P2-OB122	70	68.6	14.4	4.5	0.6	0.0	0.2	0.0	0.1	1.7	0.1	50	84	22	5	14
		C2	P2-OC23	150	60.9	18.7	9.5	1.0	0.1	0.3	0.0	0.2	3.6	0.1	100	80	32	3	30
			P2-OC24	200	73.5	15.3	3.7	0.4	0.0	0.1	0.0	0.1	1.3	0.1	37	87	21	5	11
			P2-OC25	280	62.8	18.3	8.3	1.0	0.0	0.3	0.0	0.3	4.0	0.1	110	78	30	3	34
		Rock	**Orthogneiss**	-	66.8	14.8	6.1	1.0	0.1	1.6	1.0	2.5	3.6	0.1	271	68	24	5	46
Weathered mantle on granite	**PG**	B11	P-GB131	200	67.5	14.6	6.5	1.4	0.1	0.4	0.1	0.1	1.1	0.1	46	76	24	5	10
		BC3	P-GBC31	230	65.2	16.1	6.9	1.3	0.0	0.4	0.1	0.1	1.0	0.1	43	78	26	4	9
			P-GBC32	300	59.2	16.8	11.5	1.3	0.1	0.5	0.1	0.1	1.1	0.1	51	78	32	4	10
		C3	P-GC31	330	51.7	21.4	9.6	1.5	0.1	2.6	0.3	0.2	2.0	0.1	190	79	37	2	21
			P-GC32	400	62.1	16.3	6.9	1.1	0.1	2.2	3.9	3.0	2.1	0.4	389	65	27	4	42
		Rock	**Granite**	-	61.1	17.4	6.2	1.0	0.1	1.9	3.5	3.8	3.4	0.6	416	62	28	4	56
Weathered mantle on quartzite vein	**PQ**	C4	P-QC1	30	68.5	17.5	3.9	0.4	0.0	0.1	0.0	0.1	1.9	0.0	49	90	24	4	16
			P-QC2	60	68.8	18.8	2.5	0.3	0.0	0.4	0.0	0.1	3.5	0.0	100	84	24	4	29
			P-QC3	90	69.4	16.1	5.8	0.3	0.0	0.0	0.0	0.1	2.0	0.0	45	89	24	4	16
		Rock	**Quartzite vein**	-	96.4	0.1	1.0	0.0	0.0	0.0	0.0	0.0	0.0	0.0	2	71	1	649	0

4.3. Geochemistry

4.3.1. Major Elements Contents and Related Weathering Parameters

The major element data for the weathered mantles are presented in a Table 1.

In the profiles developed on mica schist, the contents of SiO_2, alkaline and alkaline earths in decrease upward. In contrary, the abundances of Al_2O_3, Fe_2O_3 and TiO_2 increase upward. About the weathering parameters, TRB and WIP contents are decreasing upward (TRB: from 206 to 11mg.kg^{-1}; WIP: from 44 to 4%) and CIA values are above 70% (CIA: 74 - 92%) and increase upward. The silica exportation ratio above 1 (Ki: 4 - 9) and the index of lateritization (IOL) is below 30% in almost all the weathering products (IOL: 18 - 29%).

In the profiles developed on orthogneiss, SiO_2 and Fe_2O_3 show alternate increasing and decreasing contents up the profile. Like those developed on mica schist, alkaline and alkaline earths, with TiO_2 contents moderately decreases upward. On the contrary, Al_2O_3 contents increase steadily upward. The TRB and WIP values also decrease highly upward (TRB: from 271 to 37mg.kg^{-1}; WIP: from 46 to 11%) and CIA values are still above 70% (CIA: 74 - 87%). Once again, the silica exportation ratios are above 1 (Ki: 3 - 6) and the index of lateritization (IOL) is below 40% in all the weathering products (IOL: 18 - 39%).

In the profiles developed on granite, SiO_2, Fe_2O_3 and TiO_2 contents increase upward, while the abundances of alkaline and alkaline earths decrease conspicuously up the profile. The TRB and WIP values also decrease strongly upward (TRB: from 416 to 43mg.kg^{-1}; WIP: from 56 to 9%) when CIA values are above 60% (CIA: 65 - 79%). The silica exportation ratios remain above 1 (Ki: 2 - 5) and the IOL values is still below 40% (IOL: 24 - 37%) in these weathering products.

In the profiles developed on quartzite veins, SiO_2 contents decrease upward while the abundances of Al_2O_3, Fe_2O_3, TiO_2, MgO, Na_2O and K_2O increase upward. The TRB and WIP values suddenly increase upward (TRB: from 2 to 100mg.kg^{-1}; WIP: from 0 to 29%) when the CIA values are highly increase (from 84 to 90%) than the values obtained in the other weathering product. The silica exportation ratios remain above 1 (Ki: 4) and the IOL are values below 25% (IOL: 24%) in the weathering products.

In the soil profiles studied in Meïganga, major oxides behave differently. SiO_2 contents globally decrease upward in the weathering profiles from micaschists, quartzite veins, and orthogneiss, but slightly increase in granite. Al_2O_3, Fe_2O_3 and TiO_2 contents increase upward, except in the weathering profiles from granite and orthogneiss. Alkaline and alkaline earths contents decrease upward, except in the weathering profile from the quartzite veins with increasing contents. Chemical weathering parameters indicate that TRB and WIP values decrease upward in all the weathering in the exception of the weathering products developed on quartzite vein where they suddenly increase upward. Generally, the CIA values are above 65% (CIA: 65 - 92%) when the IOL do not exceed 40% and the silica exportation ratio remain above 1 (Ki: 2 - 9) in all the weathering products.

4.3.2. Trace Elements Contents

Trace element abundances (ppm) for samples collected from different soil profiles in Meïganga are presented in Table 2.

In the weathering products from micaschists, trace elements in the studied profiles show characteristics that can be generally grouped into increasing or decreasing trends. The trace element behaviors are not the same in all the profiles. In soil profiles developed on mica schist, trace elements with increasing abundance up the profile include; V, Cr, Ni, Sb, and Pb, while those with decreasing abundance up the profile include; S, Zr , Y, Nb, Ga, Hf, Sn, Mo, and U. The most abundant useful elements is Cr (63 - 289ppm), followed by Zr (85 - 268ppm), V (20 - 225ppm), Sb (1 - 62ppm), Cu (4 - 61ppm), W (9 - 44ppm), Nb (4 - 20ppm), Mo (0 - 9ppm) and Hf (2 - 5ppm).

In the weathering products from orthogneiss, trace elements with increasing contents up the soil profiles include; Y, Pb, Th, Ga, Sc, Nb, Cs, U and Mo, while trace elements showing a decrease in abundance up the profile include; S, Ba, Zr, Sr, Rb, Zn, Cu, Ni, Li, Co, Hf, W and Sn. The V and Cr display alternately decreasing and increasing contents. Useful elements contents in decreasing abundance are: Zr (215 - 383ppm), V (22 - 175ppm), Cr (62 - 170ppm), Cu (15 - 40ppm), Nb (7 - 21ppm), Hf (6 - 8ppm), Mo (2 - 5ppm) and W (1 - 3ppm).

In the weathering products from granite, most of the trace element abundances Zr, V, Cr, Y, Cu, Ni, Co, Ga, Nb, Th, Sc, Sn, Hf, U, Mo and W increase upward, while some decrease upward (Ba S, Sr, Rb, Li, Pb and Cs). Useful elements contents in decreasing abundance are: Zr (232 - 536ppm), V (116 - 175ppm), Cr (94 - 151ppm), Cu (15 - 40ppm), Nb (17 - 31ppm), Hf (5 - 11ppm), Mo (1 - 3ppm) and W (0 - 3ppm).

In the weathering products from the quartzite vein, almost all the trace elements display increasing contents. They are, in decreasing abundance: Ba, Zr, Rb, S, Cr, V, Pb, Zn, Sr, Nb , Ga, Ni, Sb, Y, Th, Cs, Cu, Li, Sc, Co, Sn, Hf, U, Mo and W. No trace of Li, Sc, Ga, Y, Nb, Cs, Hf, W, Th and U were noted in fresh rock. Useful elements contents in decreasing abundance are: Zr (135 - 182ppm), Cr (64 - 90ppm), V (29 - 66ppm), Nb (20 - 23ppm), Sb (4 - 19ppm), Cu (4 -11ppm), Hf (4ppm), Mo (1 - 2ppm) and W (2ppm).

Thus, trace elements that prevail in the Meïganga weathering products are, in decreasing order: S, Ba, Sr, Zr, Cr, V, Zn, Rb, Ni, Y, Sb, Cu, Pb, Li, Co, Ga, Nb, Th, Sc, Cs, Hf, Sn, U, Mo, and W. Traces elements enriched are: Sc, V, Cr, Sb, Cs and Pb. Trace elements depleted are: S, Rb and Sr. Useful elements that were identified in the Meïganga weathering products are, in decreasing contents: Zr (2 - 547ppm), Cr (44 - 289ppm), V (7 - 225ppm), Sb (1 - 62ppm), Cu (4 - 61ppm), Nb (4 - 31ppm), Hf (2 - 12ppm), Mo (0 - 9ppm) and W (0 - 7ppm). Thus, the most significant useful elements in the Meïganga weathering products are Zr, Cr and V.

4.3.3. REEs Contents and Fractionation

In the Meïganga weathering products, the REEs contents and related fractionation parameters are reported

in Table 3. Besides, the REEs normalized patterns of the related weathering products are shown in Figure 5.

In the weathering products from micaschists, the total contents of the REEs vary from ∑REEs: 76 to 272ppm, in which LRREs display the highest amounts (∑LREEs: 67 to 256ppm) (Table 3). The most abundant REE is Ce (29 - 110ppm), followed by La (26 - 71ppm), Nd (14 - 63ppm) and Pr (4 - 17ppm). The contents of these REEs decrease upward. Fractionation index ***a,*** vary from 5 to 16, suggesting important accumulation of LREEs in these weathering products compared to HREEs. The $(La/Yb)_N$ ratios from 5 to 44 show evidence of intense fractionation of the REEs in these weathering products. The Ce/Ce* ratios which refer to Ce anomaly vary from 0.3 to 1.2. This is consistent with both positive and negative Ce anomaly prevailing in these weathering products as confirmed by the normalization patterns in Figure 5A. The Eu/Eu* ratios related to Eu anomaly are below 1 (Eu/Eu*: 0.4 to 0.9), giving evidence of negative Eu anomaly in these weathering products as confirmed by the normalization patterns (Figure 5A). These weathering products are depleted in REEs compared to CI-Chondrite [35]. In addition, REEs are more or less highly fractionated; with fractionation intensity increasing from LREEs to HREEs as shown by the progressive scattering of the normalization patterns rightward (Figure 5A).

In the weathering products from orthogneiss, the total contents of the REEs vary from ∑REEs: 210 to 345ppm, in which LRREs display the highest amounts (∑LREEs: 189 to 316ppm) (Table 3). The most abundant REE is still Ce (72 - 130ppm), followed by La (38 - 84ppm), Nd (34 - 70ppm) and Pr (9 - 20ppm). The contents of the REEs in these weathering products increase upward. Fractionation index ***a,*** 7 to 12, suggests important accumulation of the LREEs in these weathering products compared to the HREEs.

Table 2. Trace elements contents in the Meïganga weathering profiles

				Trace elements in ppm												
	Soils profiles	**Hori-zons**	**Samples**	***Li***	***Sc***	***S***	***V***	***Cr***	***Co***	***Ni***	***Cu***	***Zn***	***Ga***	***Rb***	***Sr***	
Weathered mantle on micaschist	**P1M**	B11	P1-MB111	16	12	69	115	112	12	31	31	46	18	91	24	
		BC1	P1-MBC11	22	17	54	142	104	20	43	36	65	17	76	21	
			P1-MBC12	20	14	20	129	108	18	40	35	55	15	69	22	
		C1	P1-MC11	21	16	30	112	109	18	58	38	113	15	59	135	
	P2M	B11	P2-MB114	29	18	69	115	122	40	59	46	94	18	81	25	
		BC1	P2-MBC13	22	12	60	108	125	7	27	26	66	13	67	16	
			P2-MBC14	21	11	63	220	271	7	39	45	86	12	25	8	
		C1	P2-MC15	7	4	10	33	63	6	12	12	23	15	148	30	
	P3M	B11	P3-MB115	28	19	59	153	166	23	55	43	83	18	81	34	
		C1	P3-MC16	25	18	6	138	152	31	72	61	121	18	78	68	
		Rock	**Micaschist**	11	12	497	21	62	8	4	18	70	21	124	32	
Weathered mantle on orthogneiss	**P1O**	B11	P1-OB121	18	23	33	175	148	11	26	40	35	29	141	13	
		BC2	P1-OBC21	14	10	12	58	73	13	25	23	33	23	121	25	
			P1-OBC22	9	10	35	28	65	17	15	15	34	16	125	48	
		C2	P1-OC21	18	21	18	136	161	6	17	24	33	27	127	28	
			P1-OC22	6	6	55	22	63	9	21	20	18	15	111	73	
	P2O	B11	P2-OB122	14	11	17	61	75	11	23	22	34	22	101	17	
		C2	P2-OC23	11	26	24	147	170	7	15	29	34	29	118	20	
			P2-OC24	9	8	34	36	62	11	37	26	27	17	61	9	
			P2-OC25	9	26	5	142	158	10	14	22	27	29	114	27	
		Rock	**Orthogneiss**	28	7	6511	134	88	15	31	30	88	16	145	510	
Weathered mantle on granite	**PG**	B11	P-GB131	26	16	71	116	142	20	34	32	74	21	96	38	
		BC3	P-GBC31	28	16	48	128	112	15	35	30	70	23	90	33	
			P-GBC32	28	16	72	175	151	33	38	40	86	25	90	36	
		C3	P-GC31	51	18	70	171	99	23	37	26	147	31	181	91	
			P-GC32	35	12	70	124	94	16	14	15	89	22	144	584	
		Rock	**Granite**	38	9	1286	101	88	15	15	22	93	23	147	601	
Weathered mantle on quartzite vein	**PQ**	C4	P-QC1	8	6	80	48	90	4	19	9	40	20	94	30	
			P-QC2	6	5	64	29	64	3	11	4	51	22	150	15	
			P-QC3	9	6	103	66	81	4	19	11	39	18	87	22	
		Rock	**Quartzite vein**	0	0	10	7	44	2	6	8	3	0	1	1	

				Trace elements in ppm												
	Soils profiles	**Hori-zons**	**Samples**	***Y***	***Zr***	***Nb***	***Mo***	***Sn***	***Sb***	***Cs***	***Ba***	***Hf***	***W***	***Pb***	***Th***	***U***
Weathered mantle on micaschist	**P1M**	B11	P1-MB111	28	244	20	3	4	47	24	541	5	2	33	14	3
		BC1	P1-MBC11	33	257	15	2	3	7	12	425	5	1	19	11	3
			P1-MBC12	35	245	15	2	3	8	10	403	5	1	19	9	3
		C1	P1-MC11	34	185	9	2	3	1	2	611	4	2	39	5	2
	P2M	B11	P2-MB114	34	268	19	4	3	7	5	461	5	2	22	10	3
		BC1	P2-MBC13	25	256	19	2	3	9	11	356	5	2	19	10	3
			P2-MBC14	12	114	6	5	2	22	4	139	2	1	28	7	3
		C1	P2-MC15	11	94	14	1	4	5	29	919	3	1	9	7	2
	P3M	B11	P3-MB115	36	262	19	3	3	5	5	460	5	3	16	10	3
		C1	P3-MC16	40	222	11	1	3	2	3	585	5	2	15	6	2
		Rock	**Micaschist**	71	425	22	5	6	1	7	554	9	2	14	18	4

Weathered mantle on orthogneiss	**P1O**	B11	P1-OB121	31	314	19	5	4	0	5	297	7	3	26	29	6
		BC2	P1-OBC21	51	300	15	2	3	0	5	213	7	2	25	27	4
			P1-OBC22	54	234	8	2	2	0	6	343	6	1	44	28	4
		C2	P1-OC21	45	285	19	2	3	0	4	830	6	1	27	29	3
			P1-OC22	37	215	7	2	3	0	4	544	6	1	48	17	3
	P2O	B11	P2-OB122	47	297	15	2	3	0	5	181	7	2	21	27	4
		C2	P2-OC23	45	383	21	3	3	0	4	546	8	2	26	30	4
			P2-OC24	41	244	8	3	2	0	2	139	6	1	29	24	2
			P2-OC25	35	344	18	2	2	0	3	694	8	2	20	19	3
		Rock	**Orthogneiss**	11	547	11	1	4	0	3	1976	12	7	22	7	2
Weathered mantle on granite	**PG**	B11	P-GB131	40	536	31	2	6	1	5	404	11	3	22	25	4
		BC3	P-GBC31	42	492	30	2	6	1	5	367	10	3	21	23	4
			P-GBC32	41	425	27	3	6	1	5	524	8	2	42	22	5
		C3	P-GC31	41	232	25	1	11	0	9	1140	4	1	20	14	2
			P-GC32	21	243	17	1	7	0	7	1019	5	0	15	6	2
		Rock	**Granite**	35	233	18	1	6	0	6	1387	5	1	24	11	2
Weathered mantle on quartzite vein	**PQ**	C4	P-QC1	18	182	23	2	4	10	10	657	4	2	40	17	4
			P-QC2	15	135	23	1	4	5	13	1035	4	2	46	15	3
			P-QC3	15	157	20	2	4	19	9	586	4	2	60	15	4
		Rock	**Quartzite vein**	0	2	0	1	1	4	0	13	0	0	3	0	0

Table 3. REE contents, fractionation and normalization parameters in the Meïganga weathering profiles

				REE contents in ppm												
	Soils profiles	**Hori-zons**	**Samples**	**La**	**Ce**	**Pr**	**Nd**	**Sm**	**Eu**	**Gd**	**Tb**	**Dy**	**Ho**	**Er**	**Tm**	**Yb**	**Lu**
Weathered mantle on micaschist	**P1M**	B11	P1-MB111	52.8	95.4	13.7	51.0	8.6	1.7	6.6	0.9	5.3	1.0	2.7	0.4	2.6	0.4
		BC1	P1-MBC11	37.2	78.5	10.0	38.2	7.1	1.6	6.2	1.0	6.0	1.2	3.3	0.5	3.3	0.5
			P1-MBC12	40.1	80.3	11.4	44.6	8.6	1.9	7.4	1.2	6.9	1.4	3.7	0.5	3.5	0.5
		C1	P1-MC11	33.4	60.4	9.6	38.2	7.7	1.6	6.7	1.1	6.5	1.3	3.6	0.5	3.6	0.5
	P2M	B11	P2-MB114	41.2	109.6	10.7	40.3	7.6	1.6	6.6	1.0	6.1	1.2	3.5	0.5	3.5	0.5
		BC1	P2-MBC13	25.9	66.5	6.2	22.8	4.7	1.0	4.5	0.7	4.6	0.9	2.6	0.4	2.5	0.4
			P2-MBC14	15.9	29.1	3.8	14.4	3.1	0.7	2.7	0.4	2.5	0.5	1.4	0.2	1.4	0.2
		C1	P2-MC15	27.6	55.0	7.1	24.2	4.9	0.9	3.4	0.4	2.3	0.4	1.0	0.1	0.9	0.1
	P3M	B11	P3-MB115	41.1	94.6	10.9	42.6	8.0	1.7	7.1	1.1	6.6	1.3	3.8	0.6	3.7	0.5
		C1	P3-MC16	55.7	91.3	15.9	63.1	11.6	2.4	9.3	1.3	7.2	1.4	3.9	0.6	3.8	0.5
		Rock	**Micaschist**	40.2	89.4	11.7	45.0	10.0	2.0	9.8	1.8	12.0	2.6	7.6	1.1	7.7	1.1
Weathered mantle on orthogneiss	**P1O**	B11	P1-OB121	52.7	74.1	12.1	43.1	7.6	1.2	6.4	1.0	5.8	1.2	3.2	0.5	3.4	0.5
		BC2	P1-OBC21	71.8	112.5	18.0	64.5	12.0	1.4	10.5	1.6	9.1	1.8	4.9	0.7	4.6	0.6
			P1-OBC22	64.3	104.3	17.0	61.2	11.5	1.4	9.9	1.5	9.3	1.9	5.6	0.9	5.7	0.8
		C2	P1-OC21	83.0	130.3	19.5	70.1	11.5	1.2	9.1	1.3	7.8	1.5	4.2	0.6	3.9	0.5
			P1-OC22	67.5	71.7	14.8	49.0	8.6	1.5	7.1	1.1	7.0	1.4	3.9	0.6	3.6	0.5
	P2O	B11	P2-OB122	65.8	124.5	17.4	62.8	11.9	1.4	10.3	1.5	8.5	1.7	4.7	0.7	4.5	0.6
		C2	P2-OC23	61.0	108.9	15.1	55.3	9.4	1.1	8.1	1.2	7.5	1.5	4.3	0.6	4.1	0.6
			P2-OC24	83.7	127.0	18.7	65.0	10.3	1.5	8.4	1.1	6.8	1.4	3.8	0.6	3.7	0.5
			P2-OC25	38.0	100.5	9.3	33.9	6.1	0.7	5.4	0.8	5.6	1.2	3.6	0.5	3.6	0.5
		Rock	**Orthogneiss**	25.5	47.6	5.2	18.7	4.0	0.8	2.8	0.4	2.2	0.4	1.2	0.2	1.4	0.2
Weathered mantle on granite	**PG**	B11	P-GB131	69.6	161.7	17.8	65.0	11.4	1.9	9.4	1.3	7.7	1.4	4.0	0.6	3.8	0.5
		BC3	P-GBC31	73.0	140.6	18.6	68.8	11.6	2.0	9.3	1.3	7.8	1.5	4.2	0.6	3.9	0.6
			P-GBC32	70.4	272.9	18.4	68.2	12.0	2.2	10.5	1.4	8.0	1.5	4.0	0.6	3.8	0.5
		C3	P-GC31	91.4	147.9	22.3	83.1	14.3	3.0	11.5	1.6	8.6	1.5	3.8	0.5	3.0	0.4
			P-GC32	33.0	75.8	9.8	38.1	7.3	1.9	5.8	0.8	4.6	0.8	2.0	0.2	1.4	0.2
		Rock	**Granite**	47.6	99.4	13.2	51.7	11.4	2.1	10.2	1.6	8.5	1.4	3.0	0.3	1.8	0.2
Weathered mantle on quartzite vein	**PQ**	C4	P-QC1	47.5	98.7	12.4	44.9	8.1	1.7	6.0	0.8	4.0	0.6	1.6	0.2	1.4	0.2
			P-QC2	43.8	85.0	10.8	38.1	7.0	1.3	4.9	0.6	3.2	0.5	1.2	0.2	1.0	0.1
			P-QC3	39.1	85.8	9.8	35.7	6.6	1.4	4.9	0.6	3.3	0.5	1.3	0.2	1.1	0.2
		Rock	**Quartzite vein**	0.7	1.2	0.2	0.8	0.2	0.0	0.1	0.0	0.1	0.0	0.0	0.0	0.0	0.0

				Fractionation parameters						
	Soils profiles	**Hori-zons**	**Samples**	**∑REE**	**∑LREE**	**∑HREE**	**a**	**Ce/Ce***	**Eu/Eu***	**(La/Yb)N**
Weathered mantle on micaschist	**P1M**	B11	P1-MB111	243.0	223.1	19.9	11.2	1.1	0.8	20.3
		BC1	P1-MBC11	194.5	172.5	21.9	7.9	0.9	0.8	11.3
			P1-MBC12	212.0	186.9	25.1	7.4	0.9	1.0	11.4
		C1	P1-MC11	174.7	150.8	23.9	6.3	0.7	0.8	9.3
	P2M	B11	P2-MB114	233.7	210.8	22.9	9.2	1.2	0.8	11.9
		BC1	P2-MBC13	143.8	127.2	16.6	7.7	0.7	0.5	10.2
			P2-MBC14	76.1	66.9	9.2	7.3	0.3	0.3	11.4
		C1	P2-MC15	128.4	119.7	8.7	13.8	0.6	0.4	30.1
	P3M	B11	P3-MB115	223.5	198.8	24.6	8.1	1.2	0.9	11.1
		C1	P3-MC16	267.8	239.9	27.9	8.6	1.1	1.2	14.8
		Rock	**Micaschist**	242.0	198.3	43.7	4.5	1.1	1.0	5.3
Weathered mantle on orthogneiss	**P1O**	B11	P1-OB121	212.7	190.8	21.9	8.7	1.6	1.5	15.7
		BC2	P1-OBC21	314.0	280.2	33.8	8.3	2.4	1.7	15.7
			P1-OBC22	295.4	259.7	35.6	7.3	2.2	1.7	11.4
		C2	P1-OC21	344.6	315.7	28.9	10.9	2.7	1.5	21.5
			P1-OC22	238.2	213.0	25.2	8.5	1.5	1.8	18.6
	P2O	B11	P2-OB122	316.1	283.7	32.4	8.8	2.6	1.8	14.7
		C2	P2-OC23	278.6	250.8	27.8	9.0	2.3	1.4	13.6
			P2-OC24	332.4	306.2	26.2	11.7	2.7	1.9	18.7
			P2-OC25	210.0	188.6	21.4	8.8	2.1	0.9	8.5
		Rock	**Orthogneiss**	110.7	101.8	8.9	11.4	1.0	1.0	5.7
Weathered mantle on granite	**PG**	B11	P-GB131	356.2	327.5	28.8	11.4	1.6	0.9	18.4
		BC3	P-GBC31	343.7	314.6	29.2	10.8	1.4	0.9	18.7
			P-GBC32	474.3	444.0	30.3	14.6	2.7	1.0	18.4
		C3	P-GC31	392.8	362.0	30.8	11.8	1.5	1.4	30.6
			P-GC32	181.7	166.0	15.8	10.5	0.8	0.9	23.5
		Rock	**Granite**	252.6	225.6	27.0	8.3	1.0	1.0	26.0
Weathered mantle on quartzite vein	**PQ**	C4	P-QC1	227.9	213.2	14.7	14.5	80.9	40.4	35.0
			P-QC2	197.9	186.1	11.7	15.9	69.7	32.6	43.6
			P-QC3	190.5	178.4	12.1	14.7	70.4	33.7	34.2
		Rock	**Quartzite vein**	3.4	3.1	0.3	11.7	1.0	1.0	49.3

∑REE, sum of the rare earth elements; ∑LREE, sum of the light rare earth elements; ∑HREE, sum of the heavy rare earth elements; a, fractionation ratio of LREE vs HREE; Ce/Ce*, Ce anomaly ratio; Eu/Eu*, Eu anomaly ratio; $(La/Yb)_N$, fractionation intensity of LREE related to HREE.

The $(La/Yb)_N$ ratios from 6 to 21 give evidence of intense fractionation of the REEs in these weathering products. The Ce/Ce* ratios vary between 1.5 and 2.7. This is consistent with positive Ce anomaly prevailing in these weathering products, as confirmed by their normalization patterns (Figure 5B). The Eu/Eu* ratios are above 1 (Eu/Eu*: 1.4 to 1.9), giving evidence of positive Eu anomaly in almost all these weathering products (Figure 5B). All these weathering products are much more enriched in REEs with respect to CI-Chondrite. Thus, the REEs in these weathering products are highly fractionated compared to CI-Chondrite; but the fractionation intensity decreases from the LREEs to the HREEs as indicated by the strengthening tendency of the normalization patterns rightward (Figure 5B).

In the weathering products from granite, the total contents of the REEs vary from ∑REEs: 182 to 474ppm, in which LRREs display the highest amounts (∑LREEs: 166 to 444ppm) (Table 3). The most abundant REE remains Ce (76 - 273ppm), then La (33 - 91ppm), Nd (38 - 83ppm) and Pr (10 - 22ppm). The contents of the REEs in these weathering products increase upward. Fractionation index ***a,*** varies from 11 to 15, suggesting important accumulation of the LREEs in these weathering products. The $(La/Yb)_N$ ratios also vary from 18 to 31, giving evidence of strong fractionation of the REEs in these weathering products. The Ce/Ce* ratios vary between 1.4 and 2.7. This is consistent with strong positive Ce anomaly in these weathering products, as shown in their normalization patterns (Figure 5C). The Eu/Eu* ratios vary from Eu/Eu*: 0.9 to 1.4, indicating alternately positive and negative Eu anomaly in these weathering products (Figure 5C). These weathering products are more or less enriched in REEs with respect to CI-Chondrite (Figure 5C). Thus, REEs in these weathering products are slightly fractionated compared to CI-Chondrite (Figure 5C).

In the weathering products from the quartzite veins, the total contents of the REEs vary from ∑REEs: 191 to 228ppm, in which LRREs display the highest

amounts (∑LREEs: 178 to 213ppm) (Table 3). The most abundant REE remains Ce (85 - 99ppm), followed by La (39 - 48ppm), Nd (36 - 45ppm) and Pr (10 - 12ppm). Contents of the REEs in these weathering products strongly increase upward. Fractionation index ***a,*** varies from 15to 16, highlighting important accumulation of the LREEs in these weathering products. The $(La/Yb)_N$ ratios also vary from 34 to 44, giving evidence of strong fractionation of these REEs. The Ce/Ce* ratios vary between 69.7 and 80.9. This is consistent with strong positive Ce anomaly. The Eu/Eu* ratios vary from Eu/Eu*: 32.6 to 40.4, suggesting strong positive Eu anomaly. These weathering products are highly enriched in REEs with respect to CI-Chondrite (Figure 5D). Thus, the REEs in these weathering products are also strongly fractionated compared to the CI-Chondrite (Figure 5D).

Finally, in the Meïganga weathering products, proportions of the REEs vary from ∑REE: 76 to 474ppm, with the highest contents assigned to the LREEs (∑LREE: 67-444ppm). The most abundant REEs are in decreasing contents: Ce (29 - 273ppm), La (26 - 91ppm), Nd (14 - 83ppm) and Pr (4 - 22ppm). These REEs contents in the Meïganga weathering profiles increase upward, except in micaschist with decreasing contents upward. Thus, in the Meïganga weathering products, there is an important accumulation of the LREEs compared to the HREEs, and positive Ce and Eu anomalies, except in micaschists with negative anomalies. In Meïganga, almost all the REEs are strictly enriched in the weathering products with respect to CI-Chondrite, in the exception of those derived from micaschists in which the REEs are more or less depleted. the REEs are strongly fractionated in the weathering products, with the fractionation intensity increasing from the LREEs to the HREEs.

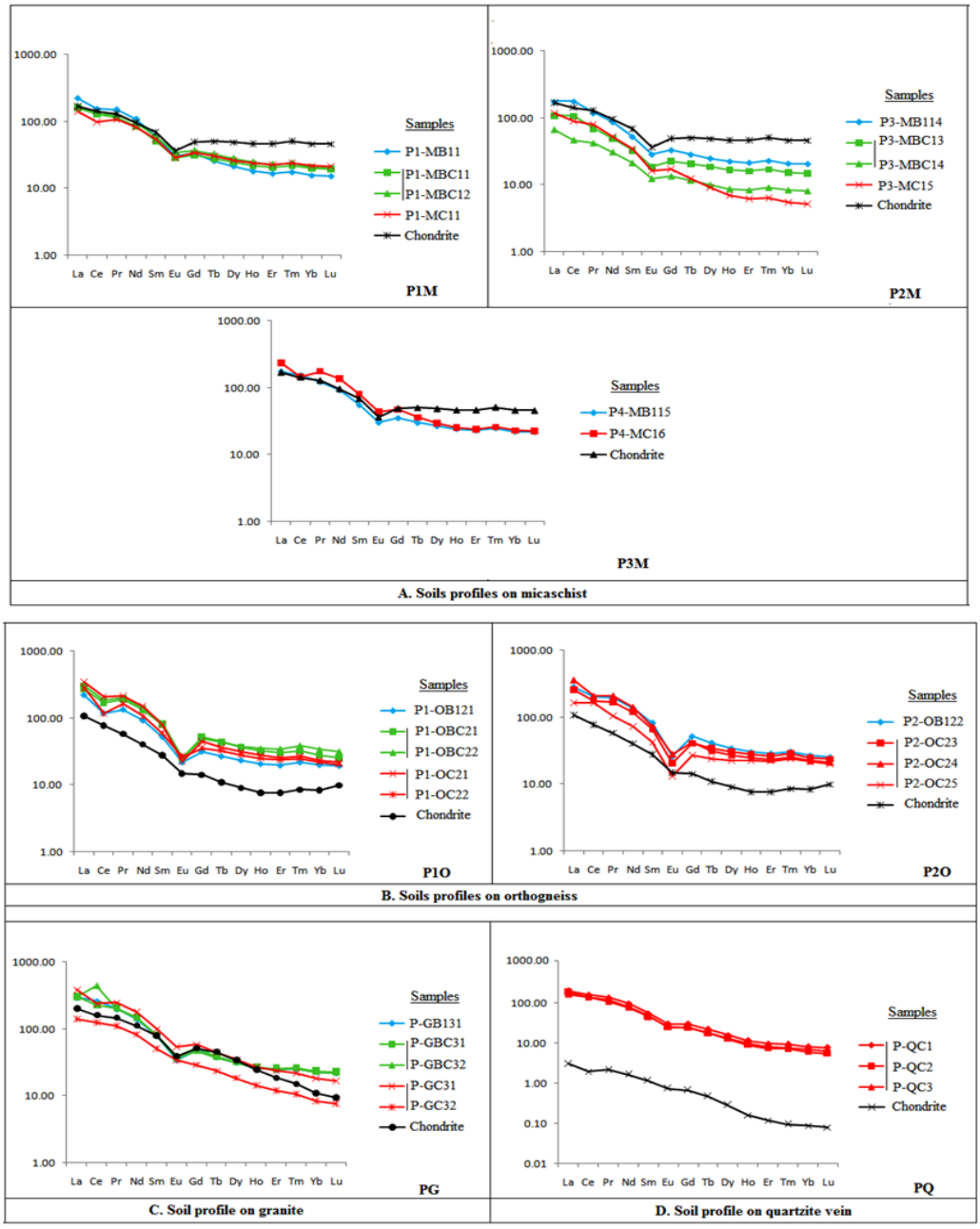

Figure 5. REEs/CI-Chondrite [35] normalized patterns in the Meïganga weathering profiles. Weathering profiles developed on: A. Micaschist; B. Orthogneiss; C. Granite; D. Quartzite vein

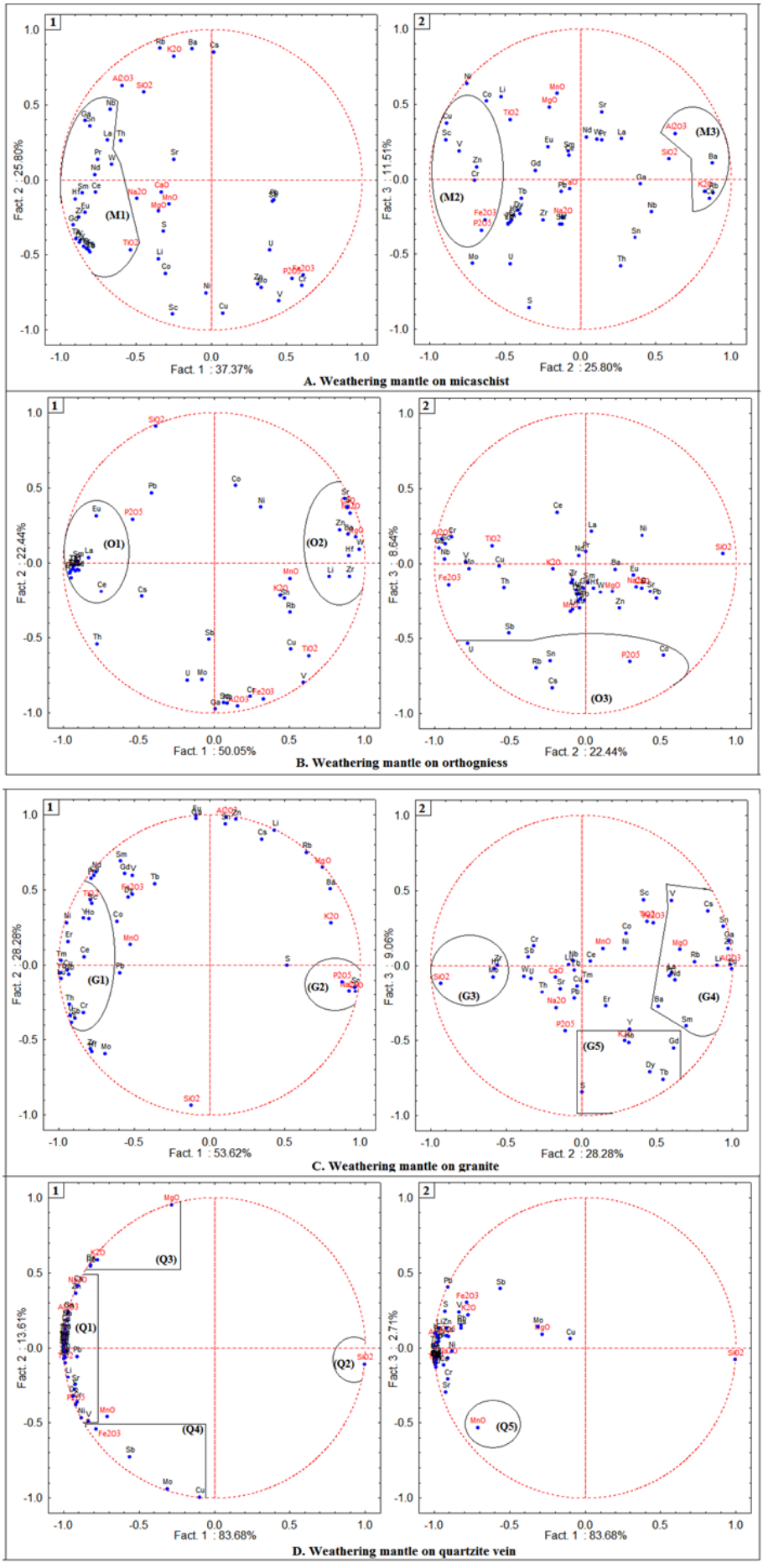

Figure 6. The PCA aggregation circles showing the relationship between major, trace and RE elements in the Meïganga weathering products, Weathering mantles developed on, A. Micaschist; B. Orthogneiss; C. Granite; D. Quartzite veins

4.3.4. Affinity between Chemical Elements

In the weathering products, the affinity between chemical elements was defined by using the principal components analysis (PCA). Consequently, the PCA aggregation circles showing the relationship between major, trace and RE elements in the samples are presented in Figure 6.

In the weathering products derived from micaschists, two major parameters (factors) accounting for 63.17% of the total variance have been defined (Figure 6A). Factor 1 expressing 37.37% of the total variance (Figure 6A1), indicates that Ga, W, Y, Sn, Hf, Zr, Nb and all the REEs are positively correlated with TiO_2, suggesting their trapping into epidote or phlogopite since TiO_2 in these minerals behave like substituting element. Factor 2 expressing 25.80% of the total variance (Figure 6A2) points out groups of variables. The first group refers to Cu, Sc, V, Zn and Cr positively correlated with Fe_2O_3 and P_2O_5, giving evidence of their likely incorporation into iron oxides (hematite or goethite), and apatite respectively. The second group is represented by Ba, Cs and Rb positively correlated with Al_2O_3 and K_2O. This may suggest that they are either trapped into clay minerals such as kaolinite or phlogopite (Al_2O_3) or simply leached during weathering (K_2O).

In the weathering products derived from orthogneiss, two principal components (factors) accounting for 72.94% of the total variance were considered (Figure 6B). Factor 1 expressing 50.05% of the total variance, reveals two groups of variables (Figure 6B1). The first group is assigned to Y and all the REEs that are strictly enriched in the weathering products, suggesting their incorporation as substituting elements or impurities into residual minerals such as zircon or titanite. The second group refers to Sr, S, Zn, Ba, W, Hf, Li and Zr positively correlated with CaO, Na_2O, MnO and MgO, giving evidence of their depletion during weathering. Factor 2 expressing 22.44% of the total variance also defines two groups of variables (Figure 6B2). The first group is represented by Cr, Nb, Ga, Sc, Th and V positively correlated with Fe_2O_3, Al_2O_3 and TiO_2, suggesting their expected incorporation into hematite or goethite; kaolinite, smectite or halloysite; and titanite or zircon respectively. The second group refers to SiO_2 that is more or less depleted, highlighting relative development of clay minerals such as smectite, halloysite or kaolinite.

In the weathering products derived from granite, two principal parameters (factors) accounting for 81.90% of the total variance were considered (Figure 6C). Factor 1 expressing 53.62% of the total variance defines two groups of variables (Figure 6C1). The first group corresponds to Cr, Sc, Ni, Cu, W, Nb, Sb, Th, U, Y, Er, Tm, Yb and Lu which are correlated positively with TiO_2 and give evidence of their likely incorporation into titanite, epidote or phlogopite.

The second group refers to Sr that is correlated positively with P_2O_5, Na_2O and CaO. Therefore, Sr in these weathering products may be leached during weathering. Factor 2 expressing 28.28% of the total variance defines two groups of variables (Figure 6C2). The first group corresponds to Zr, Mo and Hf. These elements are correlated positively with SiO_2, suggesting their trapping as substituting elements or impurities into newly formed clay minerals such as smectite or kaolinite. The second group refers to V, Cs, Sn, Ga, Zn, Rb, Li, Ba, La, Pr, Eu, Nd and Sm which are correlated positively with Al_2O_3 and MnO. This may be consistent with their incorporation into newly formed clay minerals such as smectite, kaolinite or phlogopite.

In the weathering products derived from the quartzite veins, two principal components (factors) accounting for 97.29% of the total variance were defined (Figure 6D). Factor 1 expressing 83.68% of the total variance, reveals two groups of variables (Figure 6D1). The first group refers to V, Ni, Cr, Co, S, Sr, Li, Pb, Sc, Zr, W, Y, Th, Hf, Nb, Sn, Ga, Zn, Cs and all the REEs. They are positively correlated with P_2O_5 and Na_2O, suggesting their leaching out during weathering. The second group refers to SiO_2 which is more or less depleted, favoring the development of newly formed clay minerals such as kaolinite, halloysite or smectite. Factor 2 expressing 13.61% of the total variance also defines two groups of variables (Figure 6D1). The first group corresponds to Rb and Ba positively correlated to MgO and K_2O. This may be indicative of their leaching out during weathering. The second group is represented by Sb, Mo and Cu which are positively correlated to Fe_2O_3, suggesting that they may have been trapped into residual opaque minerals.

Therefore, we have noticed that many trace elements (Ga, W, Y, Sn, Hf, Nb, Cu, Sc, V, Zn, Cr, Sb, Pb, Ni, Co, Li, Mo, Th, Rb, Cs, U, Zr and Ba), as well as almost every REEs are positively correlated with some majors elements. All the above major oxides are known to be premonitory for the presence of residual primary minerals (titanite, apatite, and zircon) or newly formed secondary minerals (phlogopite, hematite, goethite, kaolinite and smectite) in the weathering products.

4.3.5. Correlation between Major Oxides and Useful Elements

The correlation matrices between *major oxides* and identified noble metals are shown in Table 4.

Cr, Mo and U are strongly correlated with Fe_2O_3 and P_2O_5 oxides, with the correlation ratios varying from 0.87 to 0.88 for Fe_2O_3 and from 0.80 to 0.87 for P_2O_5. V, Cr, Nb and Mo are strongly correlated to Al_2O_3, Fe_2O_3 and TiO_2 oxides, with the correlation ratios from 0.86 to 0.91 for Al_2O_3, 0.81 to 0.90 for Fe_2O_3, and 0.83 to 0.91 for TiO_2 for weathering products derived from orthogneiss. V and Nb are strongly correlated with Fe_2O_3 (0.95) and TiO_2 (0.83) oxides respectively for soil developed on granite. In the weathering products derived from the quartzite veins, V, Cr, Zr, Nb, Mo, Hf, W, and U are strongly correlated to Fe_2O_3, TiO_2, P_2O_5, MnO, and Al_2O_3 oxides, with the correlation ratios varying from 0.80 to 1.00 for Fe_2O_3; 0.85 to 1.00 for TiO_2; 0.83 to 0.98 for P_2O_5; 0.92 for MnO; and 0.95 to 1.00 for Al_2O_3 respectively. Thus, according to the above correlation matrices, Cr, Mo, U, V, Nb, Zr, Sb, Hf and W, can be considered as useful elements having strong affinity (> 0.80) with major oxides like Fe_2O_3, TiO_2, P_2O_5, Al_2O_3 and MnO.

Based on the above assumption, each giving useful elements was later on used to draw up regression functions with the corresponding major elements in order to calculate the useful elements contents in each weathering product based on the major elements contents. The error factor between measured and calculated useful elements contents was used to draw up the distribution

matrices of the theoretical errors between both contents (Figure 7).

Table 4. Correlation matrix between less mobile major elements and noble metals in the Meïganga weathering products

Micaschist	SiO_2	Al_2O_3	Fe_2O_3	TiO_2	MnO	P_2O_5	Granite	SiO_2	Al_2O_3	Fe_2O_3	TiO_2	MnO	P_2O_5
V	-0.66	-0.68	0.75	0.29	0.04	0.64	**V**	-0.68	0.58	**0.95**	0.66	0.73	-0.63
Cr	-0.75	-0.77	**0.87**	-0.03	-0.04	0.78	**Cr**	0.32	-0.43	0.49	0.51	0.70	-0.70
Cu	-0.53	-0.46	0.53	0.50	0.28	0.46	**Cu**	0.07	-0.12	0.63	0.60	0.73	-0.71
Zr	0.30	0.25	-0.35	0.63	0.06	-0.31	**Zr**	0.70	-0.66	-0.01	0.46	0.16	-0.68
Nb	0.57	0.62	-0.66	0.27	0.08	-0.71	**Nb**	0.28	-0.18	0.23	**0.83**	0.20	-0.89
Mo	-0.75	-0.76	**0.87**	-0.13	-0.25	**0.88**	**Mo**	0.52	-0.63	0.32	0.15	0.61	-0.44
Sb	-0.62	-0.25	0.59	-0.26	-0.30	0.33	**Sb**	0.35	-0.42	0.49	0.48	0.64	-0.72
Hf	0.36	0.34	-0.43	0.57	0.05	-0.39	**Hf**	0.71	-0.67	-0.03	0.44	0.15	-0.65
W	0.23	0.65	-0.44	0.49	0.28	-0.55	**W**	0.51	-0.48	0.20	0.57	0.33	-0.75
U	-0.85	-0.57	**0.88**	-0.26	-0.24	**0.80**	**U**	0.39	-0.41	0.39	0.51	0.53	-0.71
Orthogneiss							**Quartzite Vein**						
V	-0.95	**0.86**	**0.90**	**0.91**	0.45	-0.54	**V**	-0.80	0.72	**1.00**	**0.85**	0.69	**0.98**
Cr	-0.85	**0.91**	**0.83**	**0.83**	0.36	-0.38	**Cr**	-0.85	0.79	**0.85**	**0.96**	**0.92**	**0.96**
Cu	-0.79	0.64	0.78	0.48	0.13	-0.54	**Cu**	0.00	-0.13	0.63	0.19	0.49	0.47
Zr	-0.42	0.22	0.31	0.74	0.53	-0.41	**Zr**	-0.98	**0.95**	**0.80**	**1.00**	0.78	**0.94**
Nb	-0.85	**0.91**	0.79	0.75	0.06	-0.32	**Nb**	-1.00	**1.00**	0.68	**0.95**	0.60	**0.84**
Mo	-0.75	0.73	**0.81**	0.19	-0.05	-0.27	**Mo**	-0.23	0.10	**0.80**	0.39	0.58	0.66
Sb	-0.56	0.38	0.61	-0.06	-0.17	-0.05	**Sb**	-0.52	0.41	**0.95**	0.59	0.52	**0.83**
Hf	-0.29	0.07	0.19	0.63	0.50	-0.34	**Hf**	-0.99	**0.98**	0.75	**0.98**	0.70	**0.90**
W	-0.31	0.03	0.24	0.54	0.48	-0.41	**W**	-0.98	**0.95**	0.79	**1.00**	0.78	**0.93**
U	-0.70	0.62	0.74	0.21	0.00	0.14	**U**	-1.00	**0.98**	**0.80**	**0.97**	0.64	**0.92**

Useful elements identified are: refractory metals (V, Cr, Zr, Nb, Mo, Hf, W); semi-precious metal (Cu); and non-precious unreactive metal (Sb)

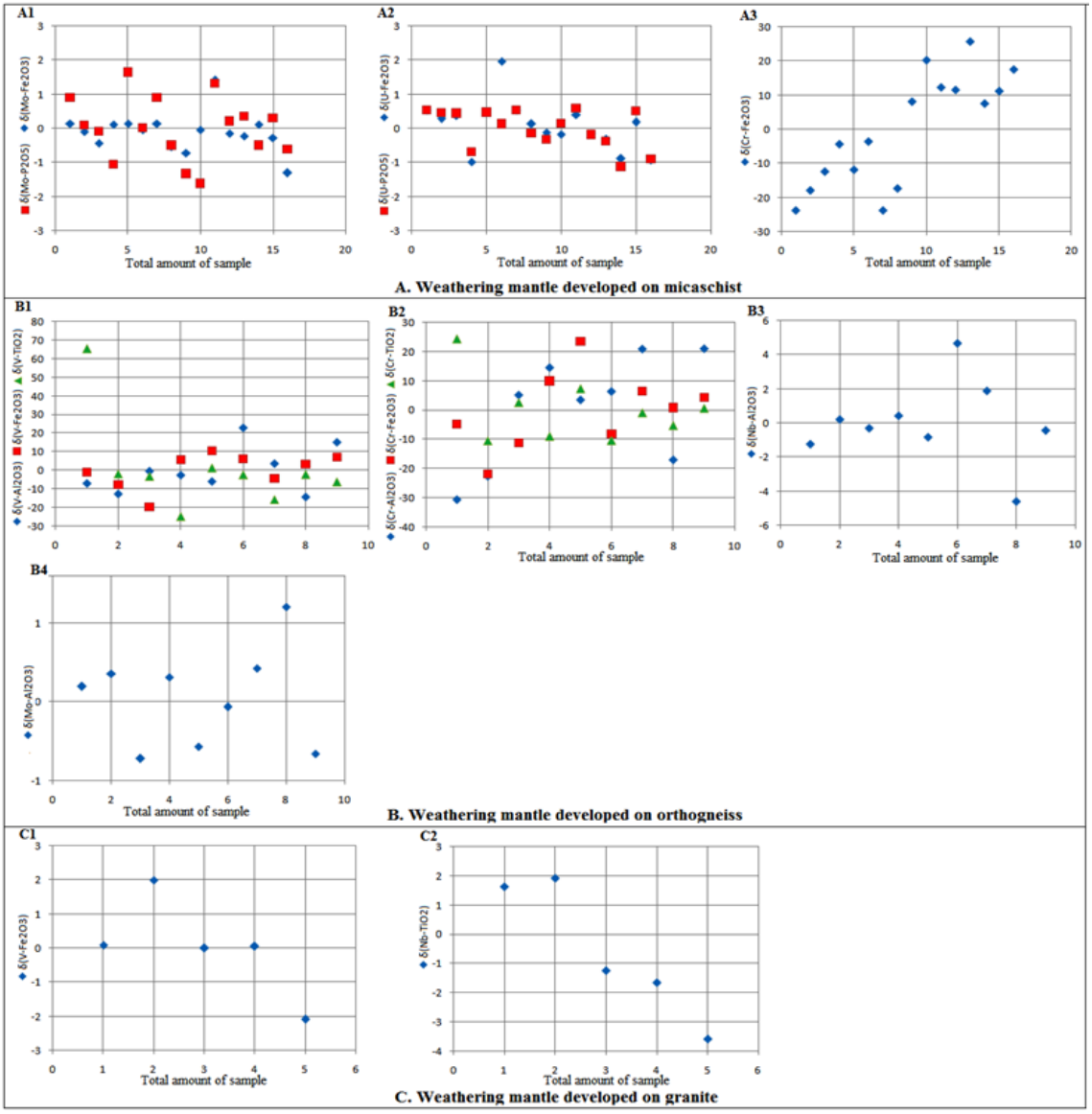

Figure 7A-C

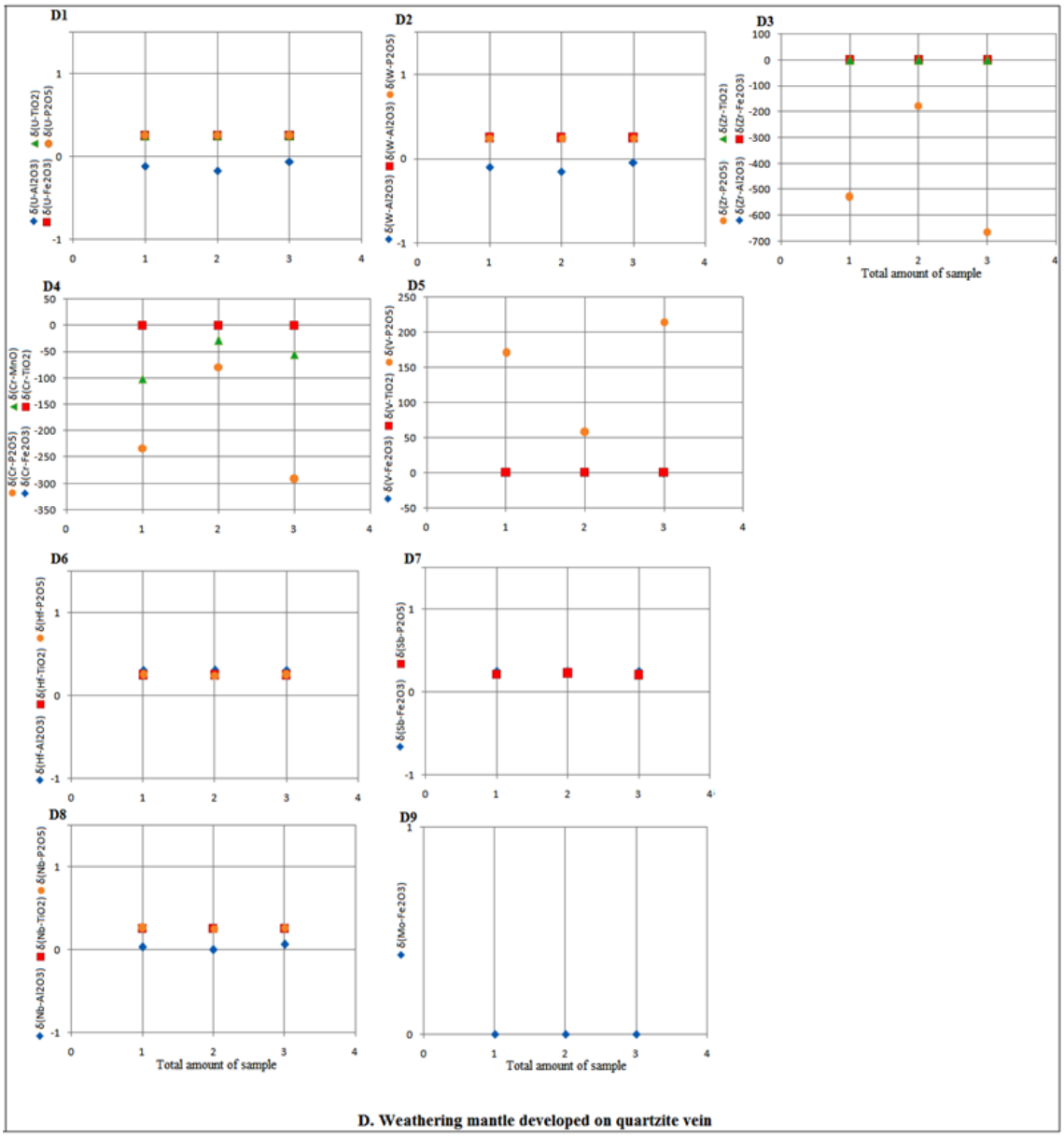

Figure 7. Distribution matrix of theoretical errors between measured and calculated useful metals contents using major elements contents in the Meïganga weathering products. *Weathering products from, A. Micaschist; B. Orthogneiss; C. Granite; D. Quartzite vein*

Hence, the must appropriated major elements that may be used to estimate, Mo and Cr contents is Fe_2O_3, and U contents is P_2O_5 for soil samples associate to micaschists. In the weathering products derived from orthogneiss, the must appropriated major elements to be used to estimate, V and Cr contents is Fe_2O_3, Nb and Mo contents is Al_2O_3. For weathering products derived from granite, Fe_2O_3 and TiO_2 are the most appropriated major elements that can be used to calculate V and Nb contents respectively. In the products derived from the quartzite veins, the most appropriated major element that can be used to calculate U, W and Nb contents is Al_2O_3; Zr and V contents are Fe_2O_3 and TiO_2; Cr contents is TiO_2; Hf contents are Al_2O_3, Fe_2O_3 and P_2O_5; Sb contents are Fe_2O_3 and P_2O_5, and Mo contents is Fe_2O_3. Definitely, in the Meïganga weathering products, major elements that can be used as tracers for the useful elements prospections are: Al_2O_3 for Nb, Mo, U, W and Hf; Fe_2O_3 for Mo, Cr, V, Zr, Hf and Sb; P_2O_3 for U, Hf and Sb; and TiO_2 for Nb, Zr, V and Cr.

5. Discussion

5.1. Weathering Pattern, Weathering Trends and Weathering Intensity in Meïganga

Rock type plays a fundamental role in weathering intensity, as well as the mobilization and concentration of chemical elements on the Earth surface. That can be used as suitable tools for analyzing and understanding trace metals concentrations in weathering products through its main evaluation parameters such as weathering pattern, weathering trend and weathering intensity [43,44,45]. This may be particularly interesting in Meïganga, a part of the mobile belt belonging to the Central African Fold Belt (CAFB) in Cameroon with varieties of mineralized rocks that has been submitted to a long-period of weathering under a hot and humid tropical climate.

Based on the weathering patterns in Meïganga, minerals association reveals high contents (up to 22.3%)

and recurrence of kaolinite as the main newly formed mineral.

Thus, in Meïganga, the prevailing rocks weathering process seem to be strong hydrolysis during which part of silica, but almost all the alkali and alkaline earth elements are leached, causing in situ crystallization of 1:1 clay minerals preferably [46,47,48]. The global increasing contents of kaolinite upward in these weathering profiles may express continuous and progressive weathering.

Also, the recurrence of smectite in the Meïganga weathering products, even in very low amounts (0.7 to 4.3%), may suggest much localized low leaching microsites that allowed crystallization of 2:1 clay minerals preferably [7,49]. In addition, the persistence of iron oxides like goethite and hematite in these weathering products (goethite: 1.9 to 13.0%; hematite: 0.5 to 8.5%), supports the fact that lateritization process occurs in this area [50,51,52]. Thus, in Meïganga, rocks have been subjected to chemical weathering (hydrolysis) under a relatively high leaching milieu that favored crystallization of 1:1 clay minerals preferably in a hot and humid tropical climate conditions, inducing low lateritization process and the development of weathered A/C or A/B/C soil profiles globally not exceeding 4 m thick.

In order to assess weathering intensity and trend in Meïganga, valuable weathering parameters (TRB, WIP, CIA, and Ki), the SiO_2-Al_2O_3-Fe_2O_3 ternary diagram of Schellmann (Figure 8A) and the Laterites classification diagram of Bardossy and Aleva (Figure 8B) were used. In the studied area, TRB and WIP parameters decrease significantly (TRB: from 416 to 11mg.kg^{-1}; WIP: from 56 to 4%) whereas these same parameters increase (TRB: from 2 to 100mg.kg^{-1}; WIP: from 0 to 29%) in the weathering products developed on quartz veins. This may be attributed to contamination by alkaline and alkaline earths during lateral migrations since the weathering profiles derived from the quartz veins are located in lowlands (around 930 m high). The CIA values above 65% (CIA: 65 - 92%), and the silica exporting ratios largely above 1 (Ki: 2 - 9) in almost all the studied soils profiles attest an intense rocks weathering in this area. This intense rock weathering may result from oscillation periods of hot and humid tropical climate with abundant rainfall (>1500 mm of annual rainfall) that has affected the Adamaoua plateau between Eocene and Holocene, keeping the subsoil into permanent humid conditions favorable to intense leaching in a well-drained milieu.

Thus, the weathering products observed in the upland between 949 and 974 m*asl* (weathering products developed on granite, micaschist, and in some extend orthogneiss) will be progressively eroded to lowland where prevailed below 933 m*asl* the weathering products developed on quartz veins. This statement may justified the alkaline and alkaline earths contamination of the weathering profiles derived from the quartz veins during lateral migrations. In fact, the weathering profile developed on quartz veins is located at the bottom of the catena and soil material present in this place is of allogenic origin (erosion of soils situated above this profile, probably micaschists).

The SiO_2-Al_2O_3-Fe_2O_3 ternary diagram of Schellmann (Figure 8A) shows that almost every weathering products are observed near the SiO_2 limit, between the kaolinization domain and the non-defined domain very close to the SiO_2 edge. Rocks weathering does not exceed the kaolinization stage. Moreover, in the Laterites classification diagram of Bardossy and Aleva (Figure 8B), almost all the Meïganga weathering products are located very closely to the Kaolinite-Hematite (Goethite) boundary, between the Kaolin and the Ferruginous Kaolin domains. Thus, kaolinization remains the major soil forming process, whatever the rock. This very early stage of lateritization known as kaolinization in Meïganga may result from progressive and continuous rejuvenation of these weathering mantles during arid periods that affected the Adamaoua plateau between Eocene and Holocene [53]. These arid periods seem to have favored an intense dissection and incision, followed by the important striping of materials by the major rivers draining this area (*Sanaga*, *Benue*, *Logone*).

5.2. Affinity between Major Oxides and Identified Useful Elements in Meïganga: Implications for Residual Mineralization Indices

Affinity between major elements and traces elements is a useful tool to better constrain the useful elements behavior during weathering, given that most of the less mobile major oxides are the main constituents of primary and newly formed secondary minerals, and useful elements are regularly incorporated within those minerals as substituting elements or impurities [54,55,56,57,58]. In the Meïganga weathering products, TiO_2, Al_2O_3, Fe_2O_3, and P_2O_5 are the major oxides known to have high affinity with identified useful elements, namely, Nb, Zr, V, Cr, Mo, U, W, Hf, and Sb. For instance, TiO_2 is closely related to Nb, Zr, V, and Cr; Al_2O_3 to Nb, Mo, U, W and Hf; Fe_2O_3 to Mo, Cr, V, Zr, Hf and Sb; and P_2O_5 to U, Hf and Sb (Figure 7). All the above major oxides controlled the presence of residual primary minerals (titanite, apatite, and zircon) or newly formed secondary minerals (phlogopite, hematite, goethite, kaolinite and smectite) in the Meïganga weathering products. The high affinity between these major oxides and identified useful elements may give evidence of their likely incorporation into the crystalline lattice of these primary or newly formed minerals [2,38,39,59,60,61,62], which can correspond to prospective mineralization indices in some weathering products. TiO_2, Al_2O_3, Fe_2O_3, and P_2O_5 oxides can be used as indicators for the identification of useful elements prospection at large scale, since their concentrations in weathering products are closely related to the associate useful elements contents.

In addition, the Meïganga weathering products derived from the quartzite veins have the highest numbers of identified useful elements: U, W, Zr, Cr, V, Hf, Sb, Nb, and Mo; followed by the weathering products from orthogneiss (V, Cr, Nb, Mo); micaschists (Mo, U, Cr); and granite (V, Nb). The weathering products with large number of useful elements proceed from weathering products (weathering products derived on quartzite veins) located at lowlands, while those with very low numbers of useful elements derived from the weathering products (weathering products derived on granite) located at the upper landscape. The increasing numbers of useful elements in lowlands may result partly from downward migration during erosion.

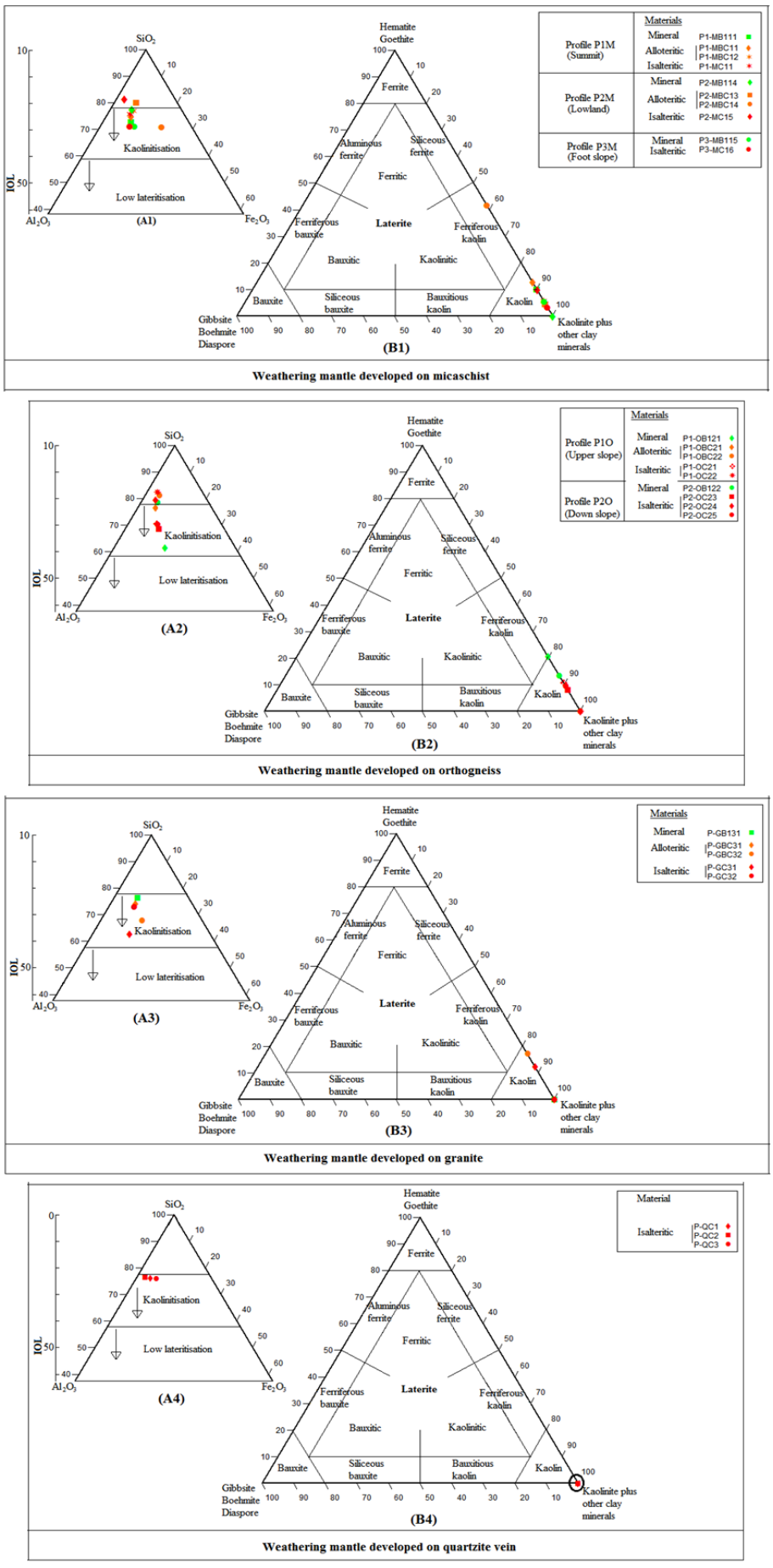

Figure 8. Weathering parameters used in the Meïganga weathering products, 8A. SiO_2-Al_2O_3-Fe_2O_3, ternary diagrams illustrating the different stages of alteration (after [52]). 8B. Classification of laterites (after [63])

Table 5. Clarks of concentrations of the identified noble metals in the Meïganga weathering products and related residual mineralization indices

		Chemical elements (ppm)	U	W	Zr	Cr	V	Hf	Sb	Nb	Mo
		Clarke (ppm)	2.7	1.25	165	102	120	3	0.2	20	1.2
Quartzite vein	Concentration of element in the sample (ppm)	Isalteritic material (Horizon C)	4	2	158	79	48	4	12	22	2
	Clarke of Concentration		**1.48**	**1.60**	**0.96**	**0.77**	**0.40**	**1.33**	**60.00**	**1.10**	**1.67**
Orthogneiss	Concentration of element in the sample (ppm)	Mineral material (Horizon B) Alloteritic material (Horizon BC) Isalteritic material (Horizon C)	-	-	-	112	118	-	-	17	4
			-	-	-	69	43	-	-	12	2
			-	-	-	123	97	-	-	15	3
	Clarke of Concentration		-	-	-	**1.10**	**0.98**	-	-	**0.85**	**3.33**
			-	-	-	**0.68**	**0.36**	-	-	**0.60**	**1.67**
			-	-	-	**1.21**	**0.81**	-	-	**0.75**	**2.50**
Micaschist	Concentration of element in the sample (ppm)	Mineral material (Horizon B) Alloteritic material (Horizon BC) Isalteritic material (Horizon C)	4	-	-	159	-	-	-	-	5
			3	-	-	152	-	-	-	-	3
			3	-	-	8	-	-	-	-	1
	Clarke of Concentration		**1.48**	-	-	**1.56**	-	-	-	-	**4.17**
			1.11	-	-	**1.49**	-	-	-	-	**2.50**
			1.11	-	-	**0.08**	-	-	-	-	**0.83**
Granite	Concentration of element in the sample (ppm)	Mineral material (Horizon B) Alloteritic material (Horizon BC) Isalteritic material (Horizon C)	-	-	-	-	116	-	-	31	-
			-	-	-	-	152	-	-	29	-
			-	-	-	-	148	-	-	21	-
	Clarke of Concentration		-	-	-	-	**0.97**	-	-	**1.55**	-
			-	-	-	-	**1.27**	-	-	**1.45**	-
			-	-	-	-	**1.23**	-	-	**1.05**	-

This downward migration may contribute to useful elements accumulation in lowlands, with expected mineralization of the corresponding weathering products [64,65,66]. It might be worth to note the extremely low or totally absent of these useful elements contents in the fresh rock (quartz veins) (V: 7 ppm; Cr: 44 ppm; Cu: 8 ppm; Zr: 2 ppm; Nb: 0 ppm; Mo: 1 ppm; Sb: 4 ppm; Hf: 0 ppm; W: 0 ppm; and U: 0 ppm) than those reported in the weathering products. This may be the consequence of the lowlands position of these weathering mantles that facilitates their migration and accumulation.

The presence of U in the weathering products derived from both quartz veins and micaschist may suggest that micaschists could be the single rock-source for U in Meïganga. Other useful elements (Cr, Mo, V, Nb, W and Hf) may have originated from orthogneiss, mica schist and granite, when Zr, and Sb seem to be inherent for the quartz veins.

Likewise, in the Meïganga weathering products, the Clarks of concentrations considered as enrichment factor for a given element compared to its concentration in the Earth crust (Clark) (Table 5), were used to assess the useful elements enrichment in the Meïganga weathering products, and thus their expected mineralization indices. So, the Clarke of concentrations of useful elements above 1 for: Sb (60.00), W (1.60), Hf (1.33), U (1.48), Mo (1.67) and Nb (1.10) in soil profile on the quartzite veins; for U (1.11 - 1.48), Cr (1.49 - 1.56) and Mo (2.50 - 4.17) in soil profiles on micaschist; for Cr (1.10 - 1.21) and Mo (1.67 - 3.33) in soil profiles on orthogneiss; and for Nb (1.05 - 1.55) and V (1.23 - 1.27) in soil profile on granite suggest their accumulation these soil profiles. Thus in Meiganga, these soil profiles may be compared to the potential domains for these useful elements to be concentrated [67]. Therefore, in the Meïganga weathering mantles, mineralization indices could be assigned to the *weathered horizon C, BC and B*. Mineralization indices in weathering products from *weathered horizons C and BC* may suggest that part of these useful elements accumulated during the first stages of weathering. In contrary, mineralization indices in weathering products from *mineral horizon B* may indicate that metals were trapped preferentially into the newly formed secondary minerals. However, in Meïganga, very low number of expected mineralization indices were reported in the weathering mantles derived from granite and orthogneiss. Considering their location in the upper landscape, this could be explained by intense erosions that affected the Adamaoua plateau, favoring the exportation of these metals from the upper landscapes to the lowlands [64,65,66]. Nevertheless, this relative accumulation of exported metals in lowlands remains transient. Their final destination seem to be the alluvial deposits along the rivers terraces in which important concentrations of these metals were reported [16,17].

6. Conclusion

In Meïganga, morphological, mineralogical and geochemical analyses of seven weathering profiles were used to understand the weathering process that may control the occurrence of mineral and chemical elements in weathering products, and eventually expected residual mineralization indices in this area. Based on the above weathering products; mineral associations; chemical elements mobility; correlation between major, trace and REEs; and affinities between major oxides and some metals lead to the following conclusions.

*(i)*Rocks have undergone chemical weathering (hydrolysis) under a relatively well-drained milieu that

favored crystallization of 1:1 clay minerals preferably in a hot and humid tropical climate conditions inducing low lateritization process and the development of weathered A/C or A/B/C soil profiles globally not exceeding 4 m thick.

*(ii)*Very early stage of lateritization known as kaolinization remains the major soil forming process, whatever the rock type. Nevertheless in Meïganga, weathering mantles are on progressive and continuous rejuvenation. The upper weathering products are progressively eroded and accumulate in the lowland position.

(iii) In the weathering products, almost all the REEs and a large number of trace elements (Ga, W, Y, Sn, Hf, Nb, Cu, Sc, V, Zn, Cr, Sb, Pb, Ni, Co, Li, Mo, Th, Rb, Cs, U, Zr and Ba) are regularly incorporated into newly formed secondary minerals and/or retained in resistant primary minerals that act like repositories, and may induce their accumulation.

(iv) In the Meïganga soil profiles, major elements that may be considered as indicators for mineralization are: TiO_2 for Nb, Zr, V, and Cr; Al_2O_3 for Nb, Mo, U, W and Hf; Fe_2O_3 for Mo, Cr, V, Zr, Hf and Sb; and P_2O_5 for U, Hf and Sb Fe_2O_3. TiO_2, Al_2O_3, Fe_2O_3, and P_2O_5 oxides have been admitted to be the main indicators for the useful elements prospection at large scale in this area, because their concentrations are closely related to the corresponding useful elements.

(v) Still in the Meïganga soil profiles, mineralization indices could be assigned to W, V, Hf, Nb, Mo, Cr, Sb and U.

(vi) weathering products with large numbers of useful elements proceed from those located at the lowlands (quartz veins), while those with very low numbers derived from the weathering products developed on rocks located at the upper landscape (micaschist, orthogneiss and granite).

References

[1] Momo, N., Yemefack, M., Tematio, P., Beauvais, A., Ambrosi, J-P., 2016. Distribution of duri crusted bauxites and laterites on the Bamiléké plateau (West Cameroon): Constraints from GIS mapping and geochemistry. *Catena*, 140, 15-23.

[2] Tematio, P., Tchaptchet, T.W., Nguetnkam, J.P., Mbog, M.B., Yongue, F.R., 2017. Mineralogical and geochemical characterization of weathering profils developed on mylonites in the Fodjomekwet-Fotouni section of the Cameroon Shear Zone (CSZ), West Cameroon. *Journal of African Earth Sciences*. 131, 32-42.

[3] Kankeu, B., Greiling, R.O., Nzenti, J.P., 2009. Pan-African strike-slip tectonics in eastern Cameroon-Magnetic fabrics (AMS) and structure in the Lom basin and its basement. *Precambrian Research* 174, 258-272.

[4] Kankeu, B., Greiling, R.O., Nzenti, J.P., Basahak, J., Hell, J.V., 2012. Strain partitioning along the Neoproterozoic Central Africa Shear zone system: structures and magnetic fabrics (AMS) from Meïganga area, Cameroun. NeuesJahrbuch fur *Geologie und Palaeontologie Abhandlungen*, 265, 27-48.

[5] Ngako, V., Affaton, P., Nnange, J.M., Njanko, T., 2003. Pan-African tectonic evolution in central and southern Cameroon: transpression and transtension during sinistral shear movements. *Journal of African Earth Sciences* 36, 207-214.

[6] Ngako, V., Affaton, P., Njonfang, E., 2008. Pan-African tectonic in northwestern Cameroon: Implication for history of westen Gondwana. *Gondwana Research* 14, 509-522.

[7] Nguetnkam, J.P., Kamga R., Villiéras, F., Ekodeck, G.E. Yvon, J., 2006. Altération du granite en zones tropicales Exemple de deux séquences étudiées au Cameroun (Afrique Centrale). *Étude et Gestion des Sols*, 14, (1), 31-41.

[8] Soba, D., Michard, A., Toteu, S.F., Norman, D.I., Penaye, J., Ngako, V., Nzenti, J.P., Dautel, D., 1991. Données Géochronologiques nouvelles (Rb-Sr, U-Pb et Sm-Nd) sur la zone mobile panafricaine de l'Est-Cameroun : âge protérozoïque supérieur de la serie de Lom. *Comptes Rendus Academie Sciences Paris* 312, 1453-1458.

[9] Toteu, S.F., Yongue Fouateu, R., Penaye, J., Tchakounté, J., Semo Mouangue, C.A., Van Schmus, R.W., Deloule, E., Stendal, H., 2006.U-Pb dating of plutonic rocks involved in the nappe tectonic in Southern Cameroon: consequence for the Pan-African orogenic evolution of the central African fold belt. *Journal of African Earth Sciences* 44, 479-493.

[10] Ebot, V., Neba, G., Suh, E., 2016. Environmental Geochemistry of Mine Tailings Soils in the Artisanal Gold Mining District of Bétaré -Oya, Cameroon. *Geochemistry Exploration Environment Analysis*, 6, 52-62.

[11] Fon, A.N., Che, V.B. and Suh, C.E., 2012. Application of Electrical Resistivity and Chargeability Data on a GIS Plat- form in Delineating Auriferous Structures in a Deeply Weathered Lateritic Terrain, Eastern Cameroon. *International Journal of Geosciences*, 3, 960-971.

[12] Freyssinet, P. H., Lecomte, P., &Edimo, A., 1989. Dispersion of gold and base metals in the Mborguene lateritic profile, East Cameroon. *Journal of Geochemical Exploration*, 32, 99-116.

[13] NtepGzeth, P., 1993. Carte de l'Or et du diamant de la province de l'Est Cameroun. Artisanaux des substances précieuses, à l'échelle de 1/500000. *DMG/MINMEE Yaoundé.*

[14] NtepGzeth P., 1994. Point sur l'exploitation artisanale des substances précieuses dans la province de l'Est-Cameroun.

[15] NtepGzeth, P., Dupuy, J., Matip, O., Fogakoh, F.A., Kalngui., E., 2001. Notice explicative de la carte thématique des ressources minérales du Cameroun.

[16] Omang, B., Bih, C., Fon, A., Embui, V., Suh, C,E., 2014. Regional Geochemical Stream Sediment Survey for Gold Exploration in the Upper Lom Basin, Eastern Cameroon. *International Journal of Geosciences*,5, 1012-1026.

[17] Omang., C.E. Suh., B. Lehmann., A. Vishiti., N.N. Chombong., A.N. Fon., J.A. Egbe., E.M. Shemang., 2015. Microchemical signature of alluvial gold from two contrasting terrains in Cameroon. *Journal of African Earth Sciences*, 112, 1-14.

[18] Suh, C.E., Lehmann B. and Mafany, G.T., 2006. Geology and Geochemical Aspects of Lode Gold Mineralization at Dimako-Mboscorro, SE Cameroon. *Geochemistry: Exploration, Environment, Analysis*, 6, 295-309.

[19] Toteu, S.F., Van Schmus, R.W., Penaye, J., Micharde, A., 2001. New U-Pb and Sm-Nd data from North-Central Cameroon and its bearing on the Pre-Pan-African history of Central Africa. *Precambrian Research*, 108, 45-73.

[20] Ufer, K., Stanjek, H., Roth, G., Dohrmann, R., Kleeberg, R., Kaufh old, S., 2008. Quantitative phase analysis of bentonites by the Rietveld method. *Clays Minerals*. 56, 272 p.

[21] Vishiti. A., Suh. C.E., Lehmann. B., Egbe. J.A., Schemang. E.M., 2015. Gold grade variation and particle microchemistry in exploration pits of the Batouri gold district, SE Cameroon. *Journal of African Earth Sciences.* 111, 1-13.

[22] Vishiti, A., Suh, C.E., Lehmann, B., Shemang, E., Ngome, N., Nshanji, N., Chinjo, F., Mongwe, O.,Egbe, A., Petersen, S., 2017. Mineral chemistry, bulk rock geochemistry, and S-isotope signature of lode‐gold mineralization in the Bétaré-Oya gold district, south‐east Cameroon. *Geological Journal*. 2017; 1-18.

[23] Herbillon, A.J., 1988. Chemical estimation of weatherable minerals presents in the diagnostic horizons of low activity clay soils. *VIIIth Int. Soil Classif. Workshop, 1986, Brazil*, 39-48.

[24] Kaiser, H. F., 1960. The application of electronic computers to factor analysis. *Educational and Psychological Measurement*, 20, 141-151.

[25] Chapman, R.J., Mortensen, J.K., 2006. Application of microchemical characterization of placer gold grains to exploration for epithermal gold mineralization in regions of poor exposure. *Journal of Geochemical*. Exploration, 91, 1-26.

[26] Chapman, R.J., Leake, R.C., Bond, D.P.G., Stedra, V., Fair grieve, B., 2009. Chemical and mineralogical signatures of gold formed in

oxidizing chloride hydrothermal systems and their significance within populations of placer gold grains collected during reconnaissance. *Economic. Geology*, 104, 563-585.

[27] Njonfang, E., Ngako, V., Moreau, C., Affaton, P., Diot, H., 2008. Restraining bends in high temperature shear zones: The « Central Cameroon Shear Zone », Central Africa. *Journal of African Earth Sciences* 52, 9-20.

[28] Ganwa, A., Frisch, W., Siebel, W., Shang K.C., Ondoa, M.J., Satir, M., Numbem, T.J., 2008. Zircon $^{207}Pb/^{206}Pb$ evaporation ages of Panafrican metasedimentary rocks in the Kombé-II area (Bafia Group, Cameroun): Constraints on protolith age and provenance. *Journal of African Earth Sciences*, 51, 77-88.

[29] Ganwa, A.A, Siebel, W., Frisch, W., Shang, C.K., 2011. Geochemistry of magmatic rocks and time constraints on deformational phases and shear zone slip in the Meïganga area, central Cameroon. *International GeologyReview*53, 759-784.

[30] Tchameni, R., Pouclet, A., Penaye, J., Ganwa, A.A., Toteu, S.F., 2006. Petrography and geochemistry of the Ngaoundéré Pan-African granitoids in Central North Cameroon: Implications for their sources and geological setting. *Journal of African Earth Sciences* 44, 511-529.

[31] Kankeu, B., Greiling, R.O., 2006. Magnetic fabrics (AMS) and transpression in the Neoproterozoic basement of Eastern Cameroon (Garga-Sarali area). *Neuesjahrbuch fur Geologie und PalaeontologieAbhandlungen*, 239, 263-287.

[32] Kankeu, B., Greiling, R.O., Nzenti, J.P., Ganno, S., Ngnotué, T., Basahak, J., Hell, J.V., 2010. Application de la technique de l'Anisotropie de la Susceptibilité Magnétique (ASM) à l'identification des structures géologiques : le cisaillement panafricain de Bétaré-Oya dans le district aurifère de l'Est Cameroun. *Annales de la faculté des Sciences, Série Sciences de la Terre* 38 (1), 17-30.

[33] Maignien, R., 1980. Manuel pour la description des sols sur le terrain. *O.R.S.T.O.M-Paris*, 145 p.

[34] Burnham and Schweyer., 2004. Trace element analysis of geological samples by inductively coupled plasma mass spectrometry at the Geoscience Laboratories: Revised capabilities due to improvements to instrumentation. *Ontario Geological Survey*, 54, 1-20.

[35] Anders and Grevesse., 1989. Abundances of the Elements: Meteoritic and Solar. *Geochimica and Cosmochimica Acta*, 53, 197-214.

[36] Nesbitt, H. W., Young, G. M., 1982. Early Proterozoic climates and plate motions inferred from major element chemistry of lutites. *Nature*, 279, 715-717.

[37] Parker, A., 1970. An index of weathering for silicate rocks. Geological Magazine 107, 501-504.

[38] Babechuck, M.G., Widdowson, M., Kamber, B. S., 2014. Quantifying chemical intensity and trace element release from two contrasting profiles, Decan Traps, India. *Chemical Geology*, 365, 56-75.

[39] Schwertmann, U., Pfab, G., 1996. Structural V and Cr in lateritic iron oxides: genetic implications. *Geochimica et Cosmochimica* Acta, 60, 4279-4283.

[40] Dempster Michael, Paul Dunlop, Andreas Scheib and Mark Cooper., 2013. Principal component analysis of the geochemistry of soil developed on till in Northern Ireland, Journal of Maps.

[41] Smee. B.W and Grunsky. E.C., 2003. Enhancements in the Interpretation of Geochemical Data using Multivariate Methods and Digital Topography. Explore - Association of Exploration Geochemists Newsletter.

[42] *Massart*, D.L. and *Kaufman*, L., *1983*. The Interpretation of Analytical Chemical Data by the Use of Cluster Analysis. John Wiley & Sons, New York.

[43] Migoń P, Lidmar-Bergström K, 2001. Deep weathering mantles and their significance for geomorphological evolution of central and northern Europe since the Mesozoic. *Earth Science Reviews, 56, 285-324.*

[44] Olvmo, M., 2010. Review of denudation processes and quantification of weathering and erosion rates at a 0.1 to 1Ma time scale. *Technical report, TR-09-18, Univ. Gothenburg, 50p*.

[45] Tijani, M.N., Okunlola, O.A., Abimbola, A.F., 2006. Lithogenic concentrations of trace metals in soils and saprolites over crystalline basement rocks: A case study from SW Nigeria. *Journal of African Earth Sciences* 46, 427-438.

[46] Dubroeucq. D., Geissert. D., Quantin. P., 1998. *Weathering* and *soil-forming processes under semi-arid conditions* in *two Mexican volcanic ash soils*. *Geoderma 86: 99-122.*

[47] Nahon, D., 1991. Introduction to the petrology of soils and chemical weathering. *A Wiley Interscience Publication*, 313 p.

[48] Shoji. S., Dahlgren. R., Nanzyo. M., 1993. Morphology of Volcanic Ash Soils. *Developments in Soil Science*, 21, 7-3.

[49] Ambrosi, J.P., Nahon, D., 1986. Petrological and geochemical differentiation of lateritie iron crust profiles. *Chemical Geology*, 57, 371-393.

[50] Aleva, 1994. Laterites: Concept, Geology, Morphology and Chemistry. *ISRIC, Wageningen the Netherlands, ISBN* 90-6672-053-0.

[51] Bitom, D., Volkoff, B., Abessolo, M., 2003. Evolution and alteration in situ of massive iron duricrust in Central Africa. *Journal of African Earth Sciences*, 37, 99-101.

[52] Schellmann, W., 1981. Considerations on the definition and classification of laterites. Proceedings of the International Seminar on Lateritisation Processes, IGCP 129 and IAGC, Trivandrum, India. *Oxford and IBH Publishing Company, New Delhi*, 1-10.

[53] Grimaud, J. L., 2014. Dynamique long-terme de l'érosion en contexte cratonique : l'Afrique de l'Ouest depuis l'Eocène (Thèse de Doctorat). *Université Toulouse III Paul Sabatier*, 302p.

[54] Beauvais and Roquin., 1996. Petrological differentiation patterns and geomorphic distribution of ferricretes in Central Africa. *Geoderma*, 73, 63-82.

[55] Lopez, J.M.G., Bauluz, B., Fernandez, C., Oliete A.Y., 2005. Factors controlling the trace element distribution in fine-grained rocks: the Albian kaolinite-rich deposits of the Oliete Basin (NE Spain). *Chemical Geology*, 214, 1-19.

[56] Nacir El Moutouakkil and BoubkerBoukili., 2015. Interactions chimiques au niveau d'une interface micacée : cas des phlogopites magmatiques zonées de la minette de l'île de Jersey. *Bulletin de la Société Royale des Sciences de Liège*, 84, 175 - 193.

[57] Ndjigui P.-D., Badinane B.F.M., Nyeck B., Nandjip K.H.P., Bilong, P., 2013. Mineralogical and geochemical features of the coarse saprolite developed on orthogneiss in the SW of Yaoundé. *Journal of African Earth Sciences* 79, 125-142.

[58] Onana, V.l., Donald Ntouala, R.F., Tang, S.N., Effoudou, E.N., Kamgang, V.K., Ekodeck, G.E., 2016. Major, trace and REE geochemistry in contraghsted chlorite schist weathering profiles from southern Cameroon: Influence of the Nyong and Dja Rivers water table fluctuations in geochemical evolution processes, *Journal of African Earth Sciences*.

[59] Etame, J., Bilong, P., Bitom, D., Robain, H., Volkoff, B., Belinga, S.M., 1998. Relation sol jaune et sol rouge dans une sequence de sols sur gneiss en zone forestière du Cameroun. *Sci. Technol. Dév.*, 6, 1, pp. 29-37.

[60] Mbenoun, A., Ngon Ngon, G., Bayiga, E., Yongue Fouateu, R., Bilong, P., 2013. Gold Behavior in Weathering Products of Quartz Vein in Mintom Area South Cameroon (Central Africa). *International Journal of Geosciences*, 4, 1401-1410

[61] Nguetnkam, J.P., Kamga, R., Villieras, F., Ekodeck, G.E., Yvon, J., 2007. Pedogenic formation of smectites in a vertisol developed from granitic rock from Kaele (Cameroon, Central Africa). *Clay Miner*. 42, 486-501.

[62] Zarasvandi, A., Carranza, E.J.M., Ellahi, S.S., 2012. Geological, geochemical and mineralogical characteristics of the Deh-now bauxite deposits, Zagros fold betl, Iran. *Ore geology reviews*, 48, 125-138.

[63] Bardossy and Aleva., 1990. Lateritic bauxites. *"Developments in Economic Geology," Elsevier, Amsterdam*, 27, 624.

[64] Colin and Viellard., 1991. Behavior of gold in the lateritic equatorial environment: weathering and surface dispersion of residual gold particles, at Dondo Mobi, Gabon. *Applied Geochemistry, 6, 279-290*

[65] Ekengélé, N.L., Sabine, D.D., Philémon, Z.Z., Jung, M.C., 2016. Physical and Metals Impact of Traditional Gold Mining on Soils in Kombo-Laka Area (Meïganga, Cameroon). *International Journal of Geosciences*, 7, 1102-1121.

[66] Lacal, J., Da Silva, P.; Garci, R. ; Sevilla, M. T. ; Procopio, J. R. ; Hernandez, L., 2003. Study of fractionation and potential mobility of metal in sludge from pyrite mining and affected river sediments: changes in mobility over time and use of artificial ageing as a tool in environmental impact assessment. *Environmental Pollution*, 124, 291-305.

[67] Bouragba et Chabou., 2015. Etude des minéralisations de la chaîne des Azerou (Bibans, Bordj Bou Arreridji). *1ères Journées Nationales d'étude sur les Géosciences, Université Ferhat Abbas. Résumé*, 62-63.